International Ocean Colour Science Meeting 2019 | Advancing Global Ocean Colour Observations

High-Temporal Resolution Capabilities Discussion
1400 Overview (Joe Salisbury, Wonkook Kim)
1410 Questions (Antonio Mannino, Maria Tzortziou, Chuanmin Hu, ZhongPing Lee, Joe Salisbury)

High-Spatial Resolution Capabilities Discussion
1450 Overview (Arnold Dekker)
1500 Questions (Nima Pahlevan, Joe Ortiz, Chuanmin Hu, ZhongPing Lee, Eric Hochberg)

Combined High-Spatial/High-Temporal Resolution Capabilities
1540 Overview (Maria Tzortziou)
1550 Questions (Arnold Dekker, Nima Pahlevan, Joe Ortiz, Chuanmin Hu, ZhongPing Lee, Eric Hochberg, Joe Salisbury, Antonio Mannino, Wonkook Kim)

International Ocean Colour Science Meeting 2019 | Advancing Global Ocean Colour Observations

What Geostationary data brings to the table

- More data and far less bias in averaging

- Particle and solute dynamics in complex advective regimes
  (sediments, phytoplankton. pollution)

- Growth and decline of biogeochemical stocks e.g. $\delta_{STOCK} / \delta\tau$

- Variable illumination and phytoplankton responses

More data and less averaging bias in the Baltic Sea

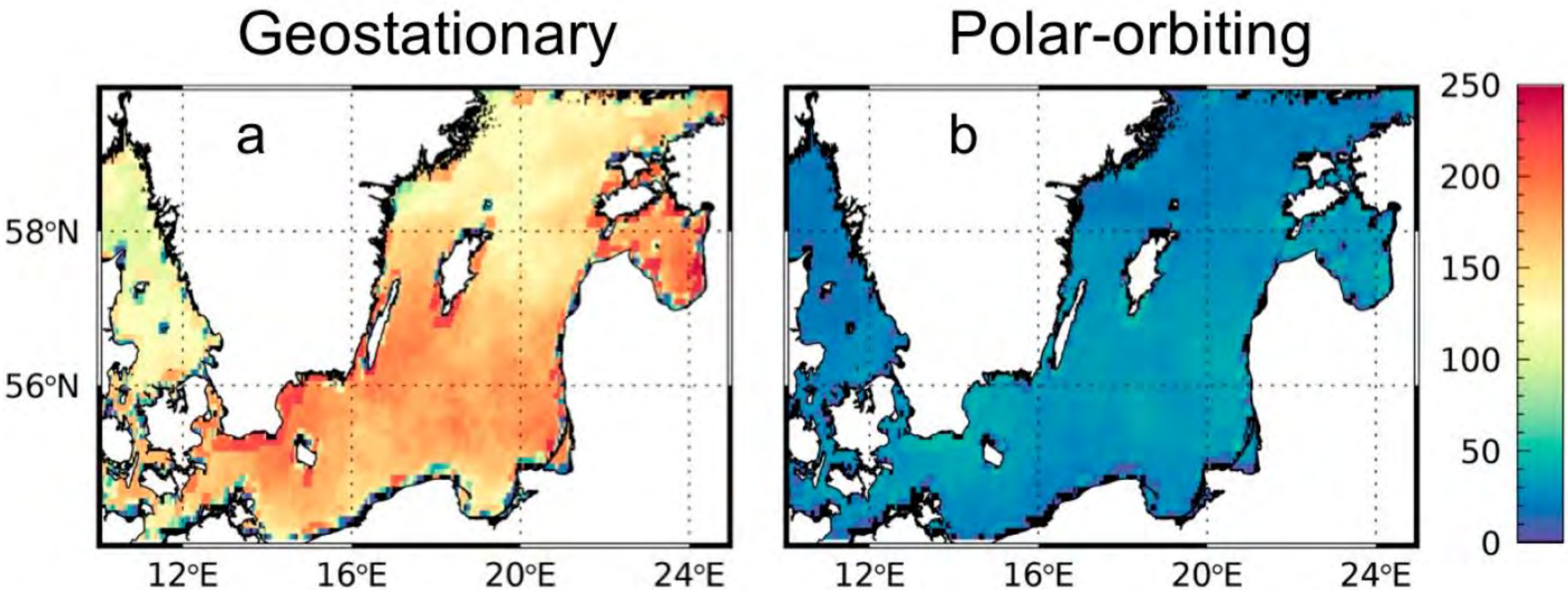

Figure 5. Number of valid observations in case of GEO (**a**) and LEO (**b**) in May 2016. Observations with solar zenith angles greater than 70° were excluded.

Bellichio et al, 2018

Particle and solute behavior at native timescales:
Tidal behavior of suspended sediment

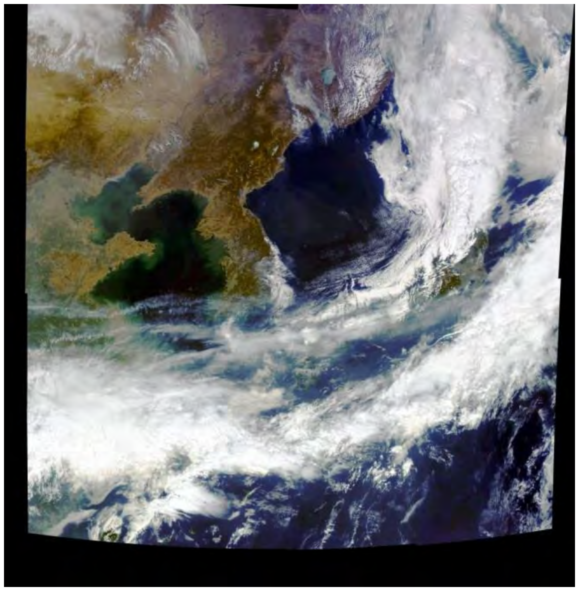

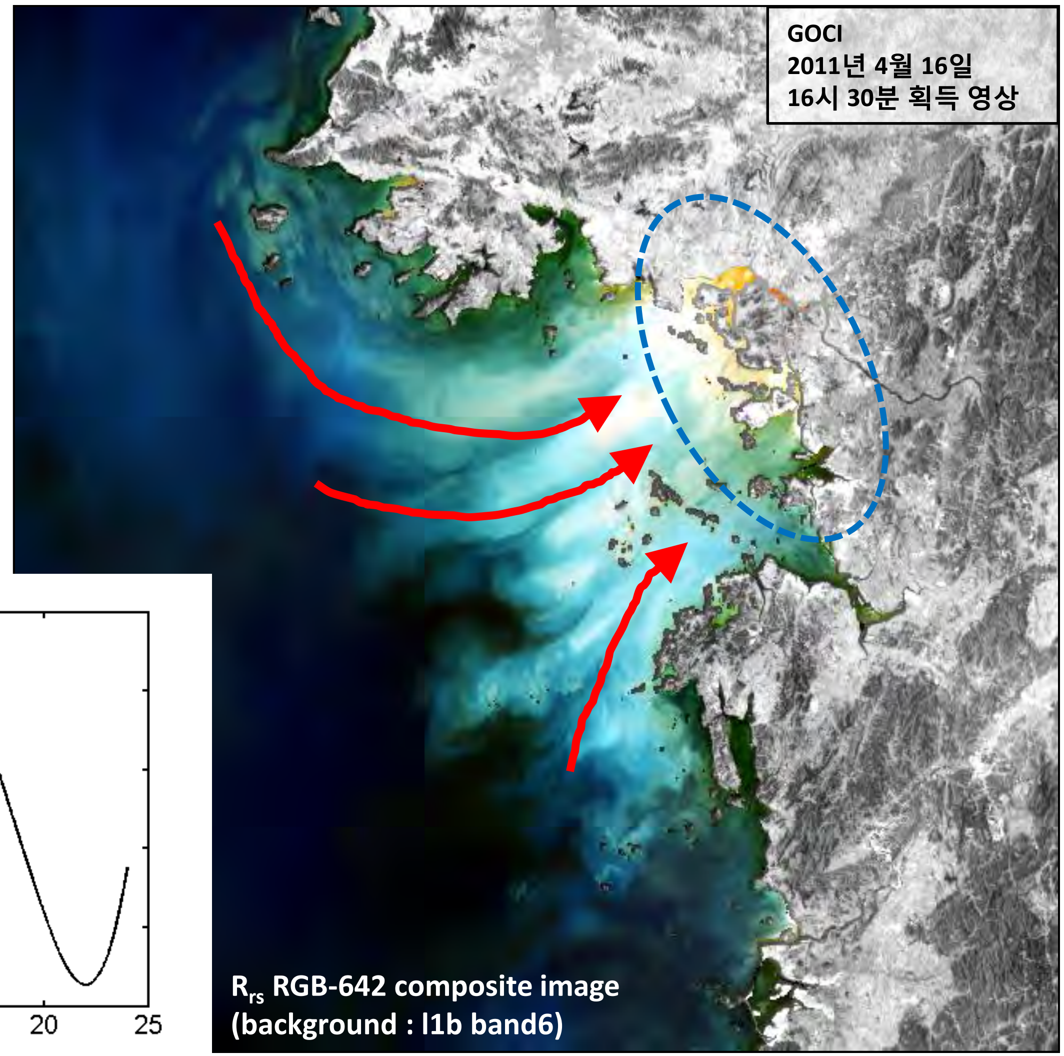

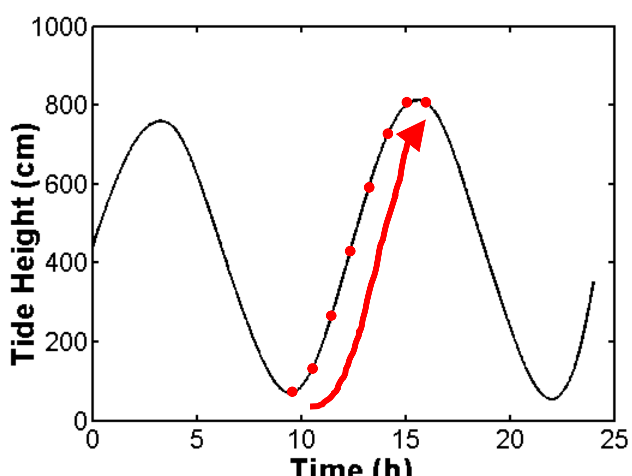

Particle and solute behavior at native timescales: Ocean dumping busted by the GOCI police

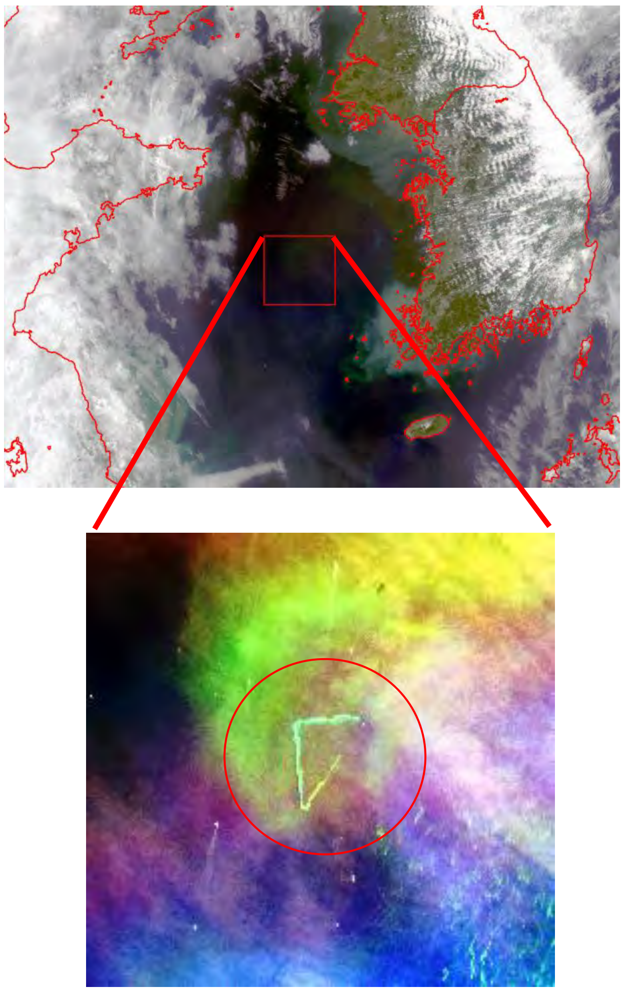

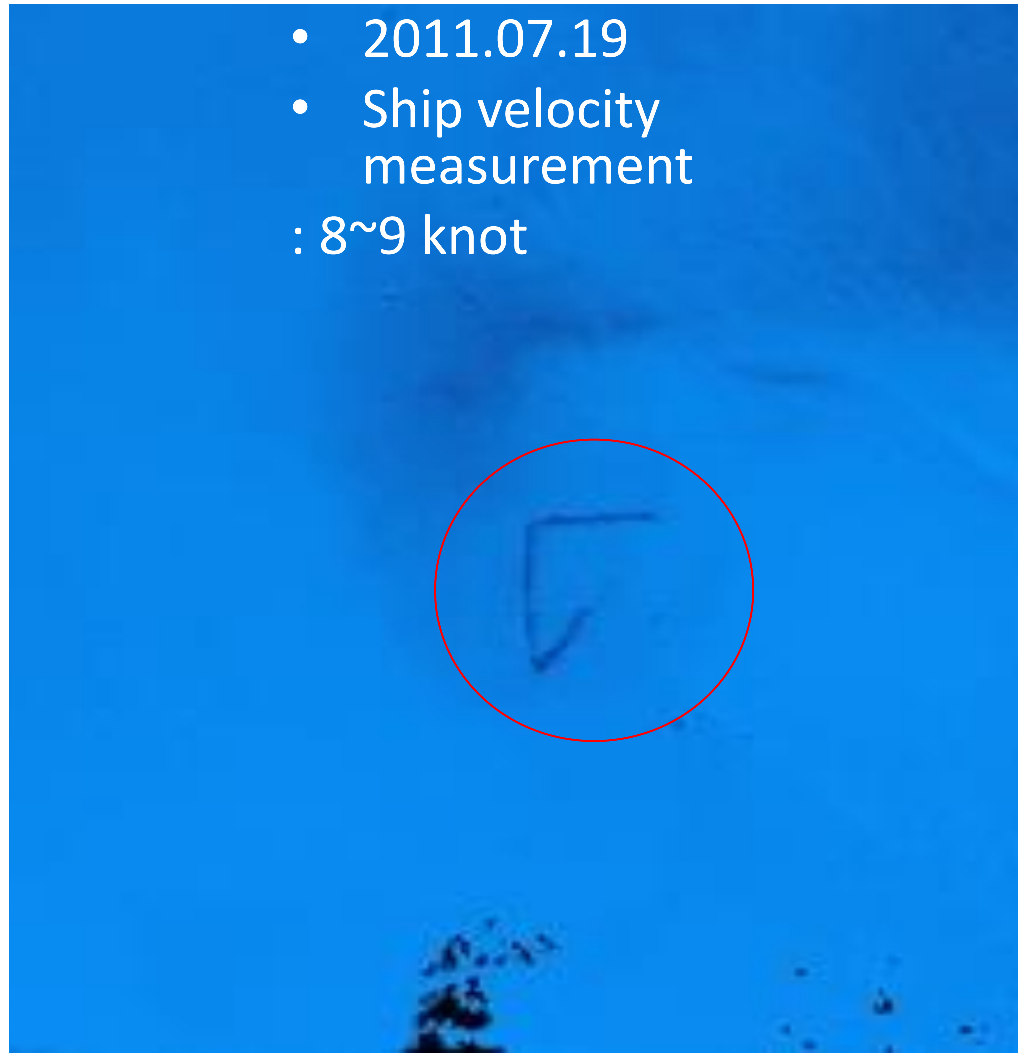

Growth and decline of biogeochemical stocks:
Changes of cyanobacterial bloom possibly due to vertical migration

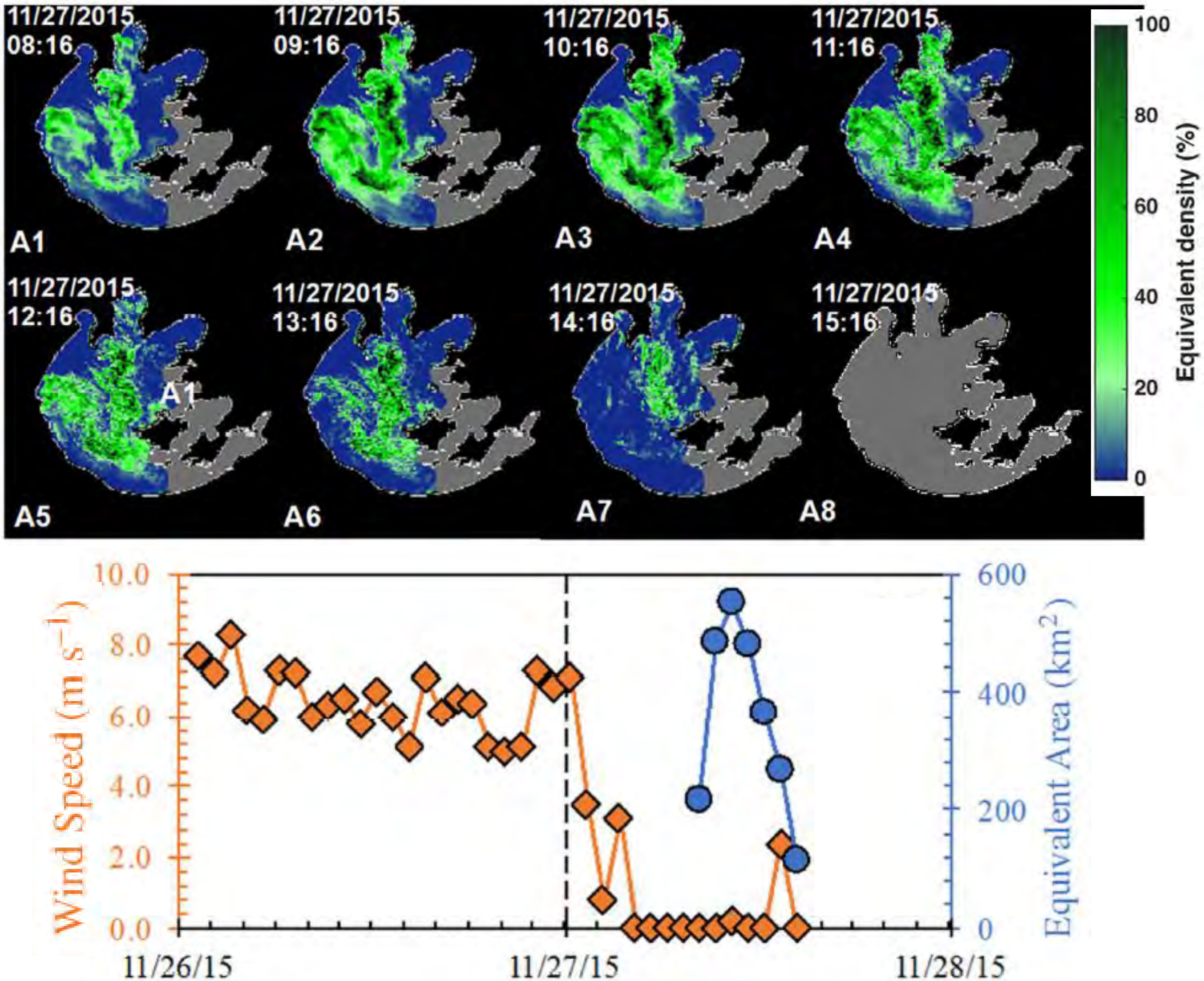

(Qi et al., 2018, L&O)

Variable illumination and phytoplankton responses
Can GOCI data be used to retrieve photosynthetic parameters?

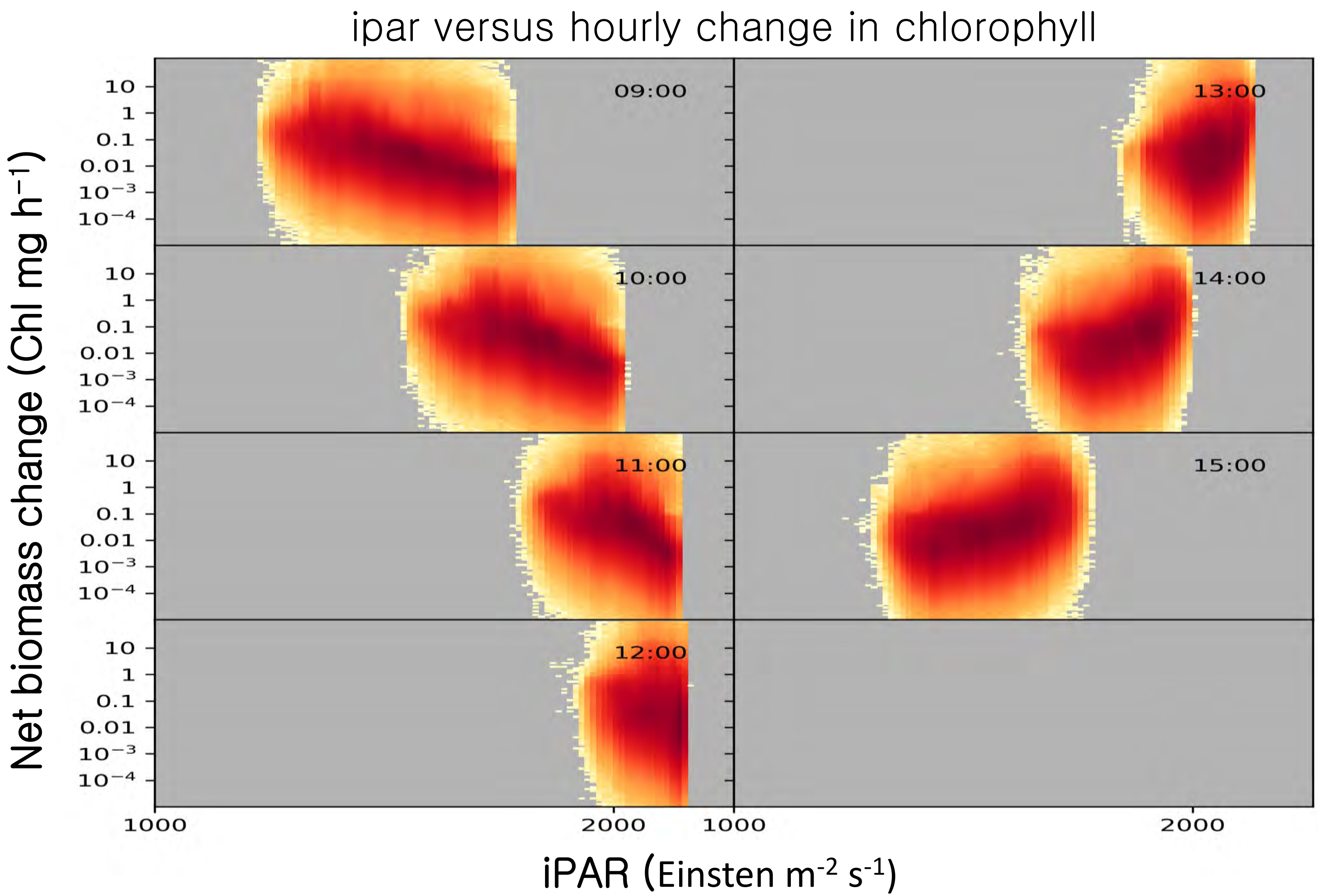

Salisbury, Jonsson, Mannino, Kim et al.

International Ocean Colour Science Meeting 2019 | Advancing Global Ocean Colour Observations

Slides from co-convener Wonkook Kim

Submesoscale turbulence statistics from GOCI

1. Velocity field from **“hourly”** GOCI images
   - Using Particle Image Velocimetry (PIV) technique

PIV-derived (4km resolution)

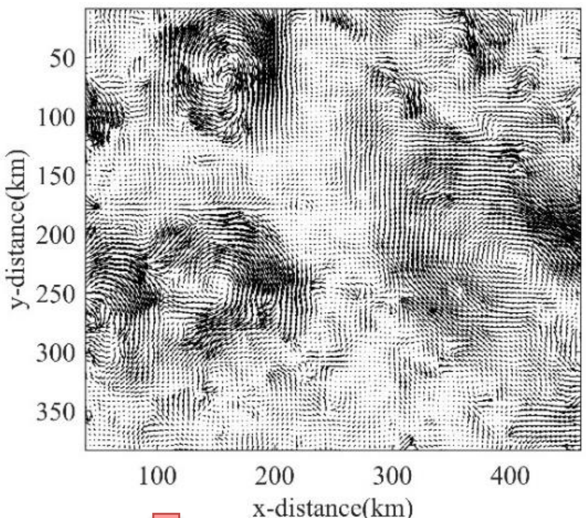

AVISO (25km resolution)

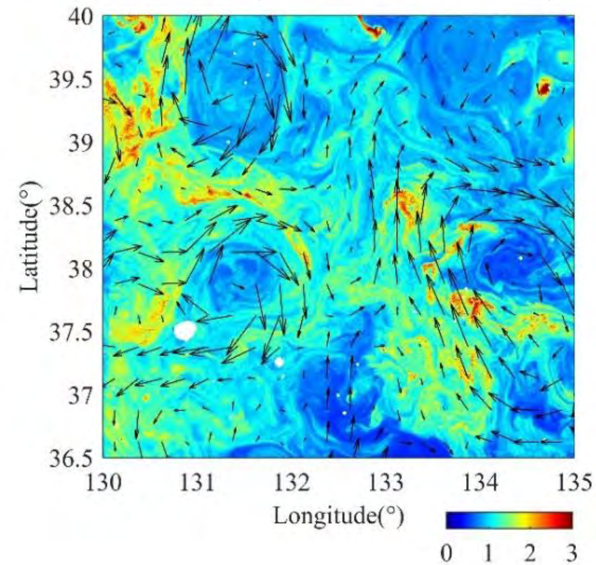

Choi, Park, & Kim
(submitted to GRL)

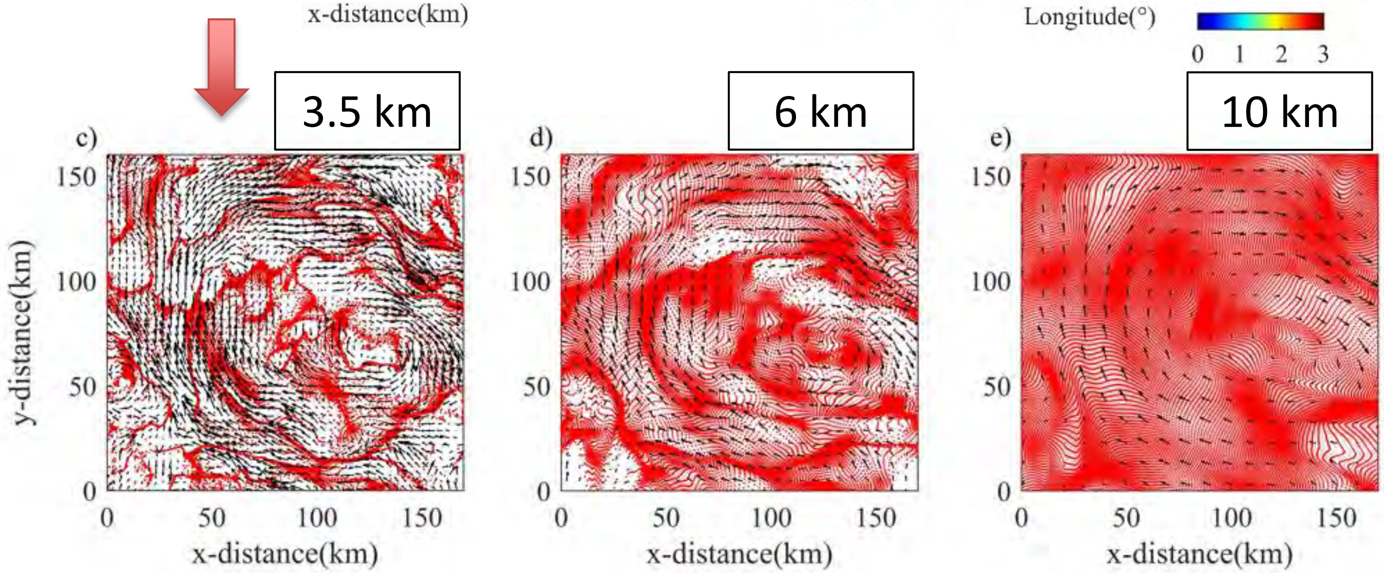

Derivation of surface velocity from GOCI using MCC

*MCC : Maximum cross correlation

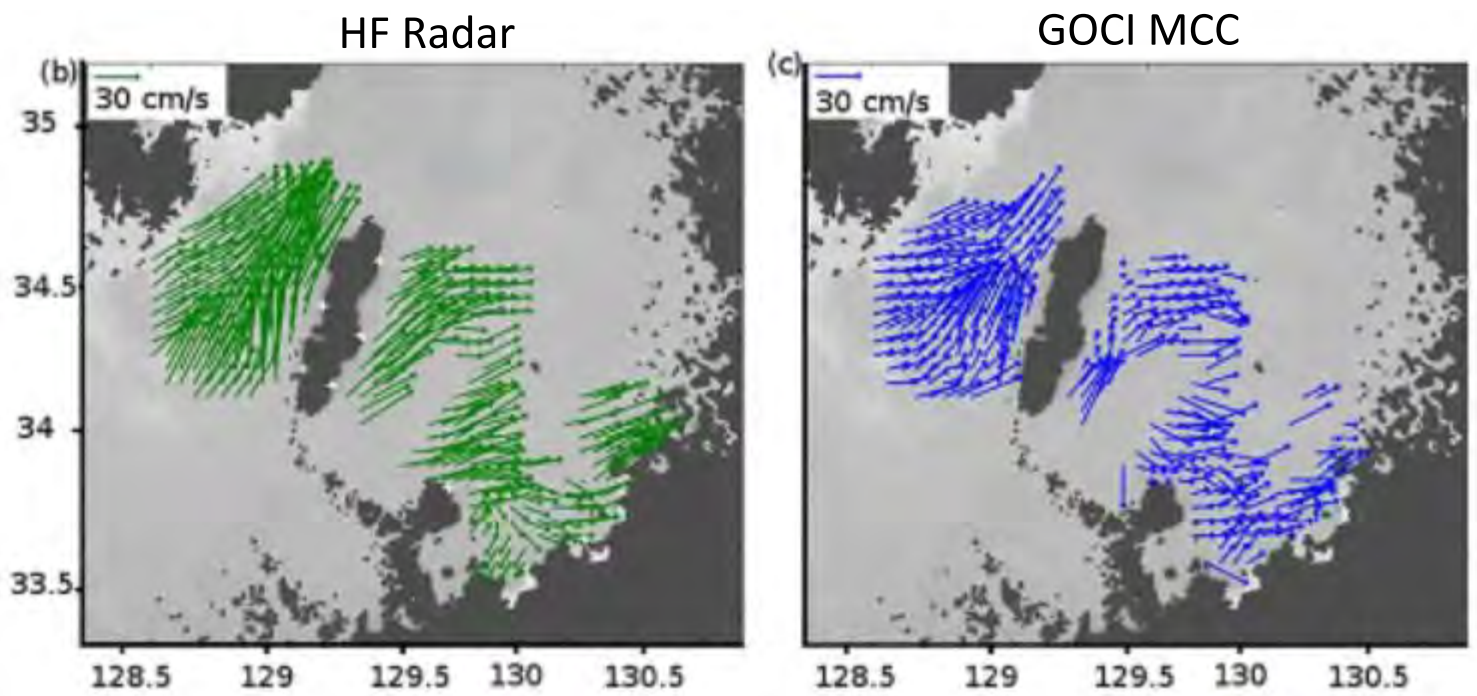

Warren et al., 2016

Submesoscale turbulence statistics from GOCI

2. Kinetic energy spectra and structure function

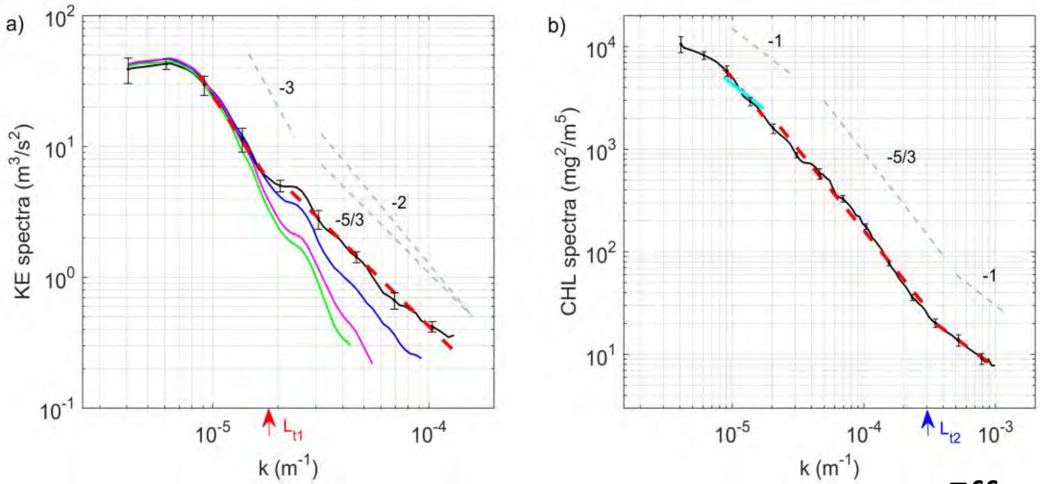

Figure 2. (a) Two-dimensional azimuthally averaged kinetic energy with difference resolutions of 3.5 (black), 5 (blue), 8 (purple), and 10 (green) km. The slopes of the best fitting lines in red correspond to 2.51 above L_{t1} and 1.62 below L_{t1}; **(b)** two-dimensional azimuthally averaged Chla spectra. The best fitting lines at difference scale ranges (120km ~ 55km, 45km ~ 3.5km, and 3km ~ 1km from left to right) correspond to the slopes of -1.55, -1.58, and -0.94, respectively

Effective resolution of altimeter (Ballarotta et al, 2019)

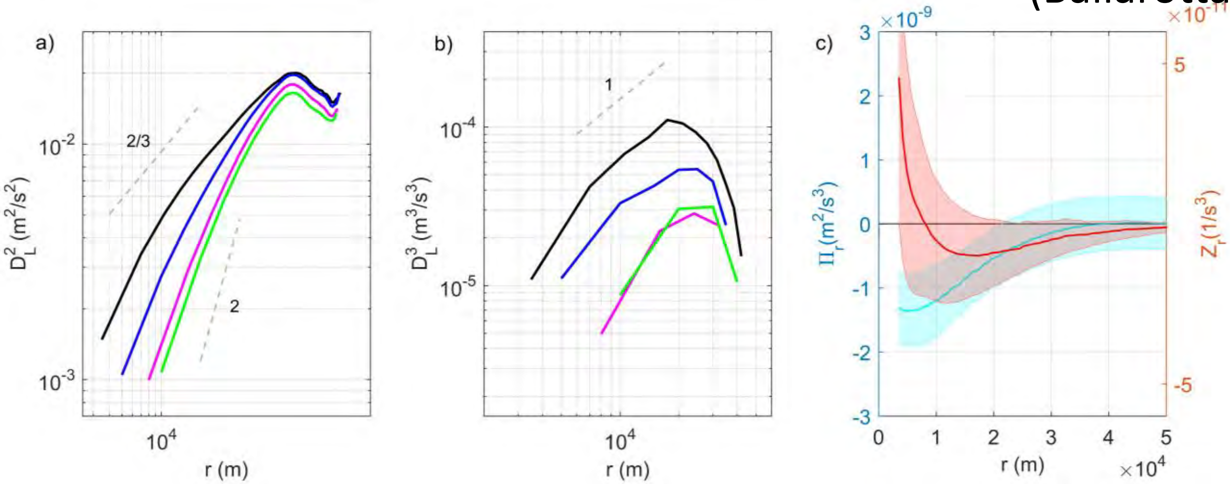

Figure 3. (a) Second-order longitudinal structure functions with difference resolutions of 3.5 (black), 5 (blue), 8 (purple), and 10 (green) km; **(b)** third-order longitudinal structure functions; **(c)** fluxes of kinetic energy Π_r (cyan) and enstrophy Z_r (red), where r denotes a cutoff length scale of low-pass filter with Gaussian kernel. Shaded areas indicate standard deviations.

Choi, Park, & Kim (submitted to GRL)

Diurnal variability of red tide

1. Southern Coast of Korea
   - July 26th , 2018
   - Using RBR algorithm (Noh et al., 2018) applied to GOCI hourly images
   - Species: *Cochlodinium Polykrikoides*

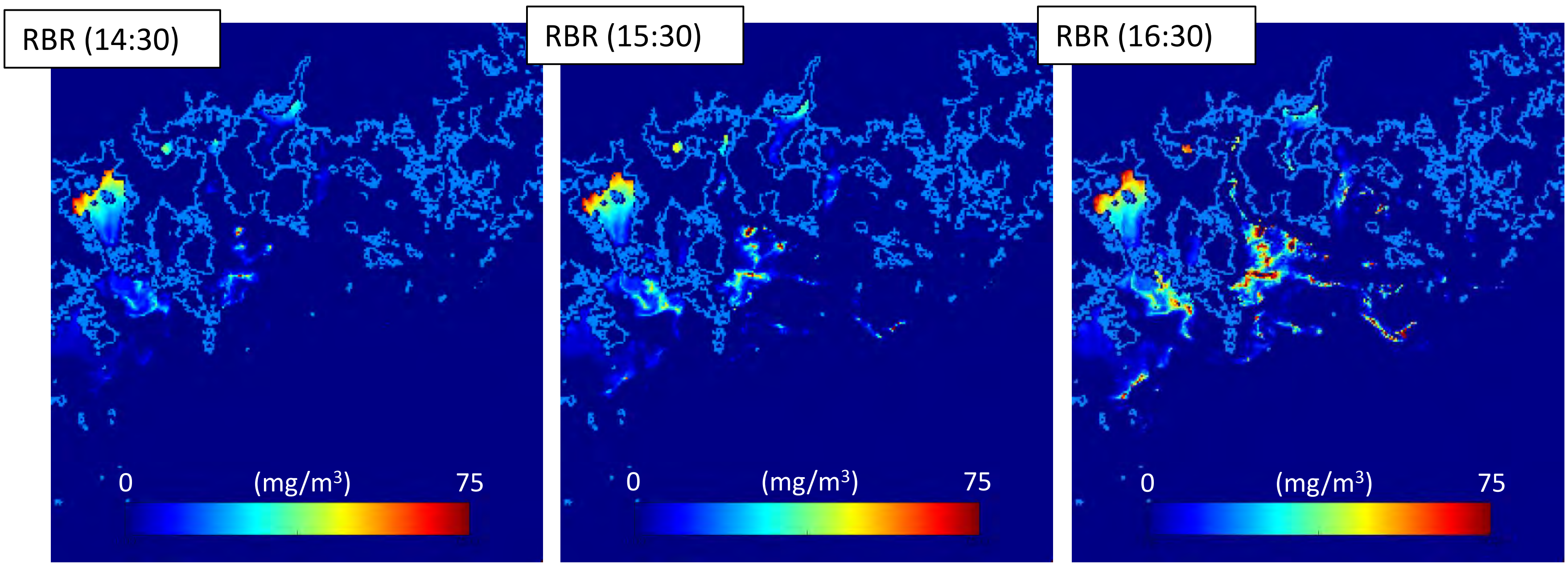

Acknowledge to MOF R/D project "Establishment and demonstration of red tide detection and prediction system for minimizing red tide damage" (PI: Donhyug Kang) and Korea Ocean Satellite Center, KIOST

High Temporal Applications - Focus Points

1. Successful utilization of current or planned high temporal resolution observations (ABI, HIMIWARI-8, GOCI-1, China GEO?)

2. How can existing or planned, high temporal resolution observational capabilities be utilized in the study of the open ocean and its margin systems?

3. New science enabled by high frequency ocean color observations.

4. What challenges, limitations or uncertainties are associated with the usage of high temporal remote sensing observations and what gaps exist in current or planned remote sensing infrastructure?

Sea Ice (3-15 Jan 2011)

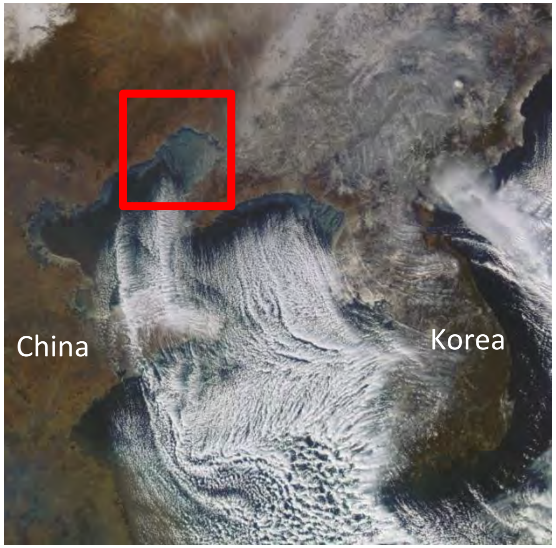

- Acquisition by GOCI from 03 to 15 Jan 2011
- As temperature dropping, area of sea ice widen and sea ice thicken

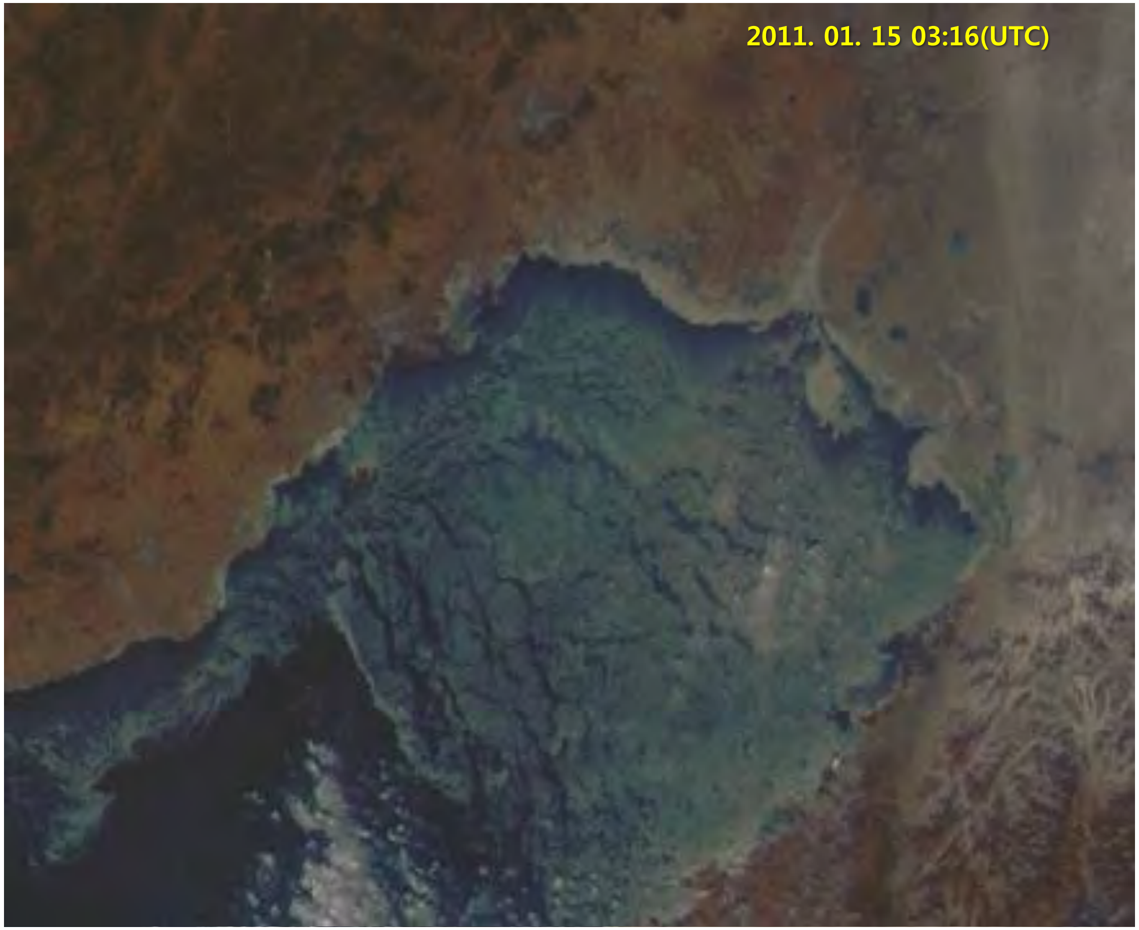

New science enabled by better daily averaging

SEVIRI daily composite of 34 images
Quasi cloudfree

MODIS: 1 image
60% clouded

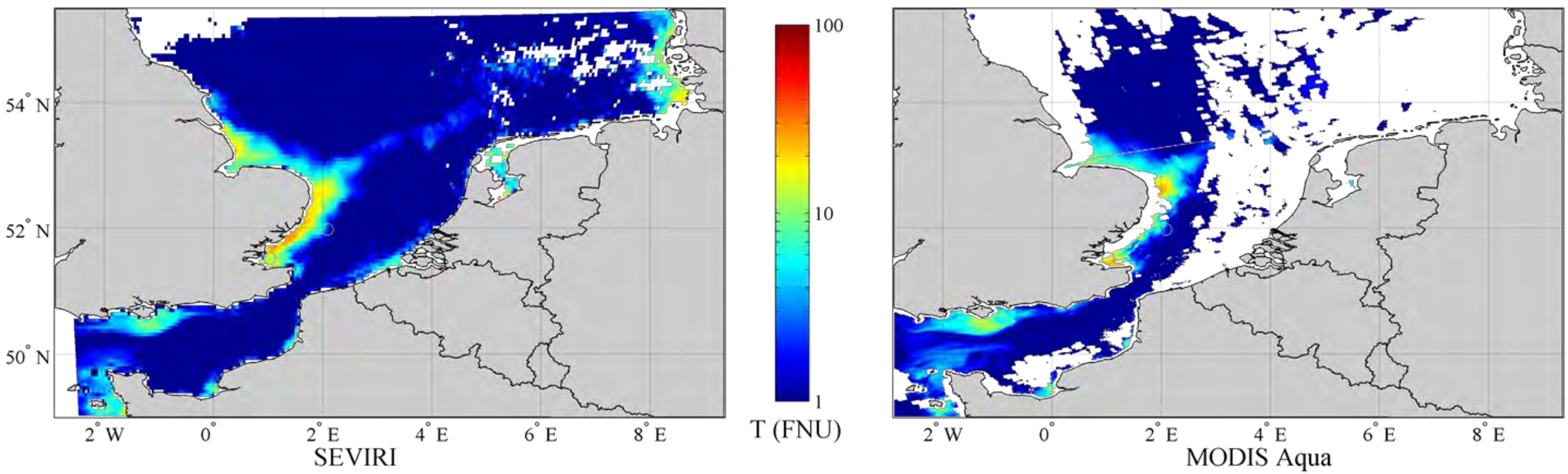

Neukermans, G. 2012

More data

Enhanced temporal resolution: GEO versus LEO

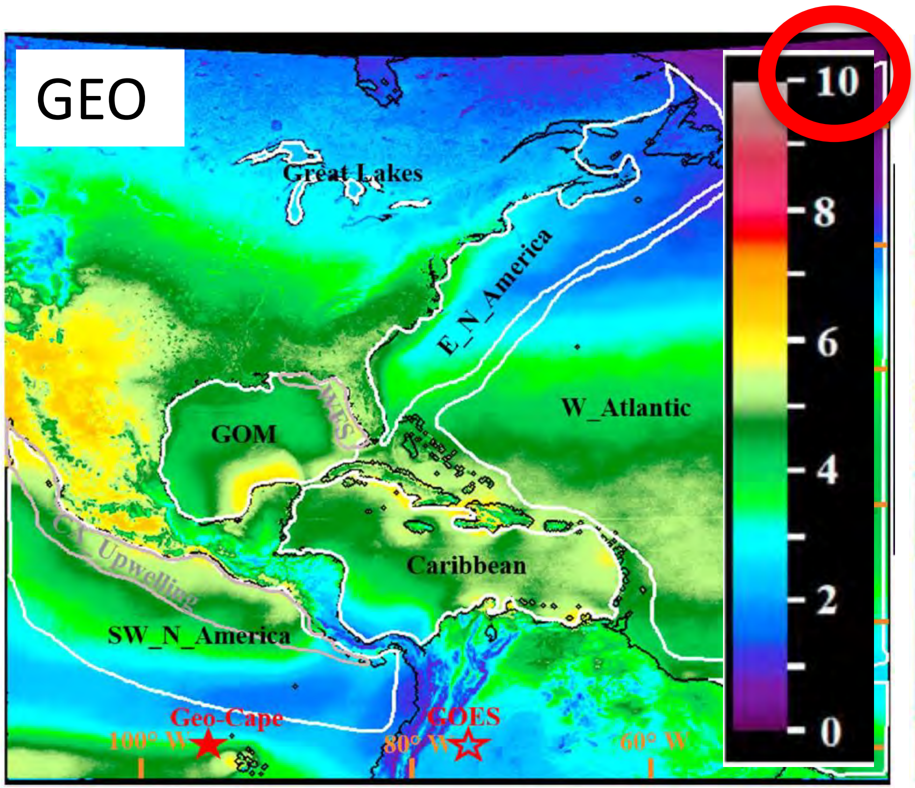

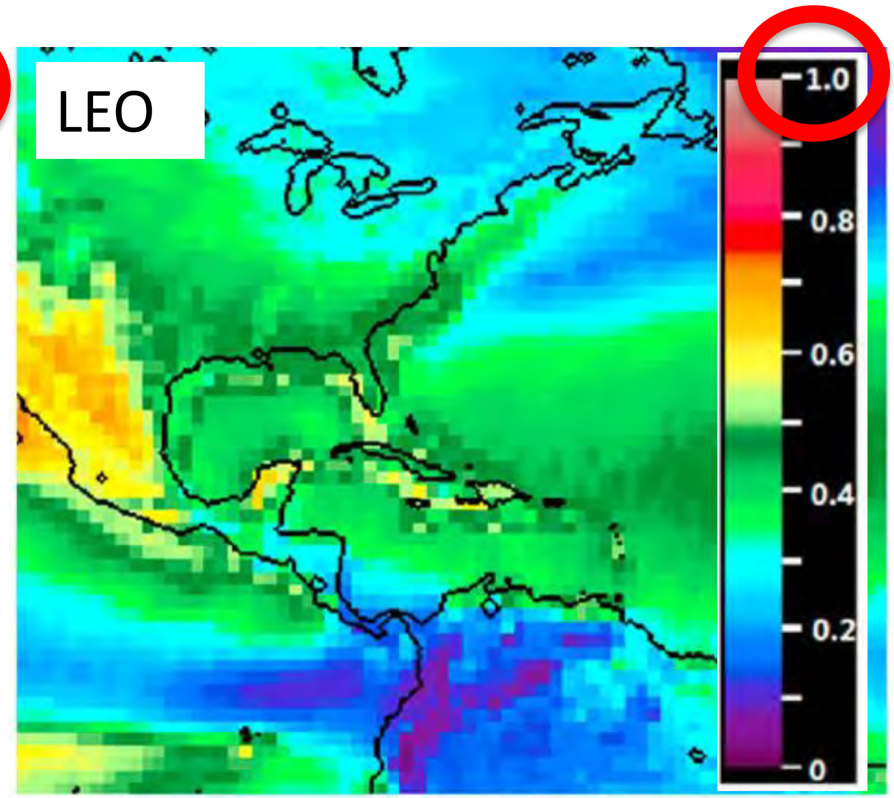

# of cloudfree observations in a typical day (Feng et al., 2017)

September 12, 2006 Time sequence of 710 nm:
Diurnal migration of the bloom?

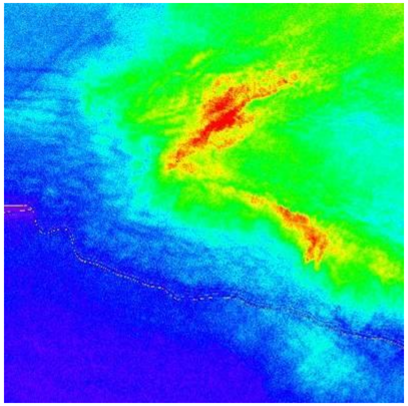

0908

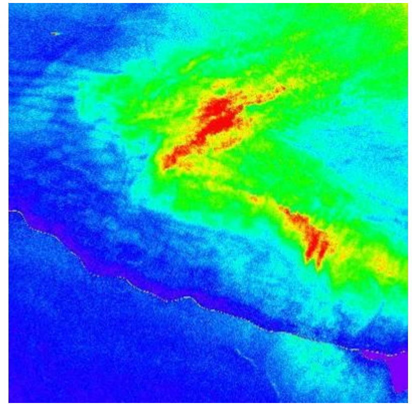

0938

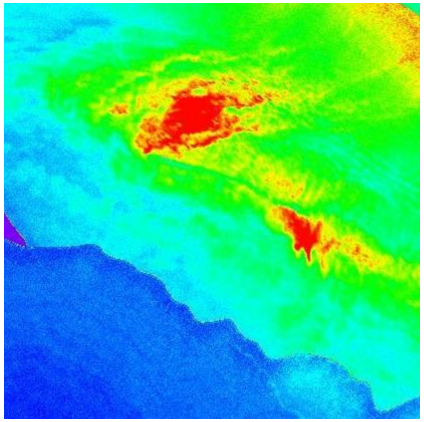

1006

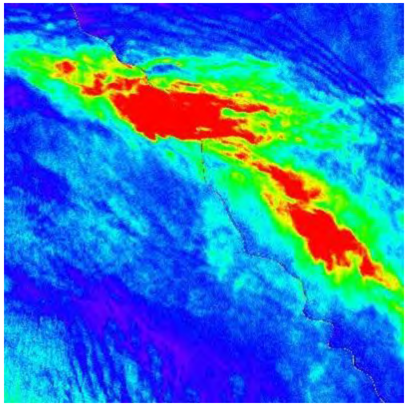

1124

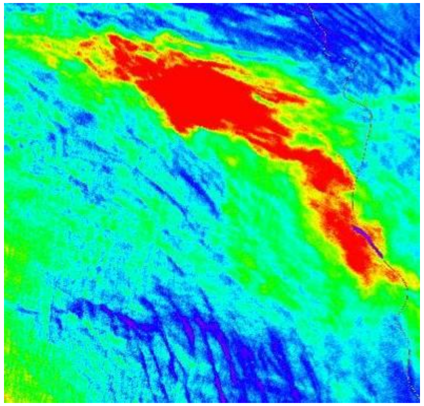

1204

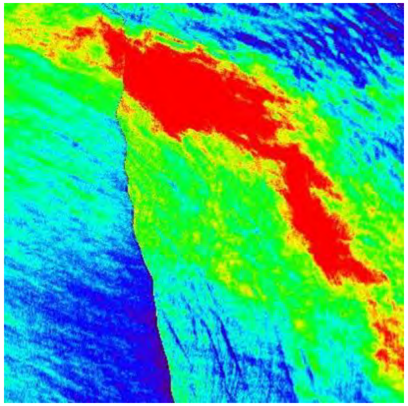

1238

images by Maria Kavanaugh

Without GEO, we would miss:

AERONET-OC184, MTRI Hyperspectral spectrometer (Sept 19, 2016) and NOAA MODIS CI (Sept 20 2016)

KSU VPCA Spectral decomposition **CyanoHAB** and **Green algae** from:

- AERONET-OC184
- MTRI hyperspectral spectrometer

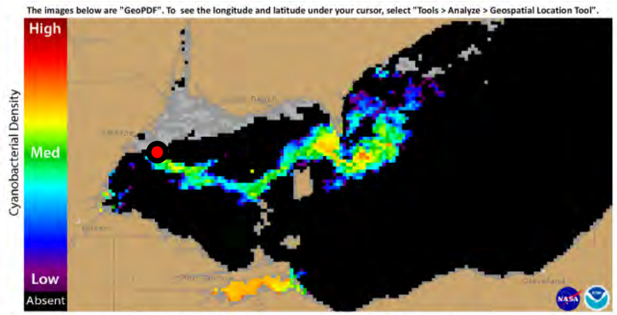

Figure 1. Cyanobacterial Index from NASA's MODIS-Aqua data collected 20 September, 2016 at 2:32 EDT. Grey indicates clouds or missing data. The estimated threshold for cyanobacteria detection is 20,000 cells/mL.

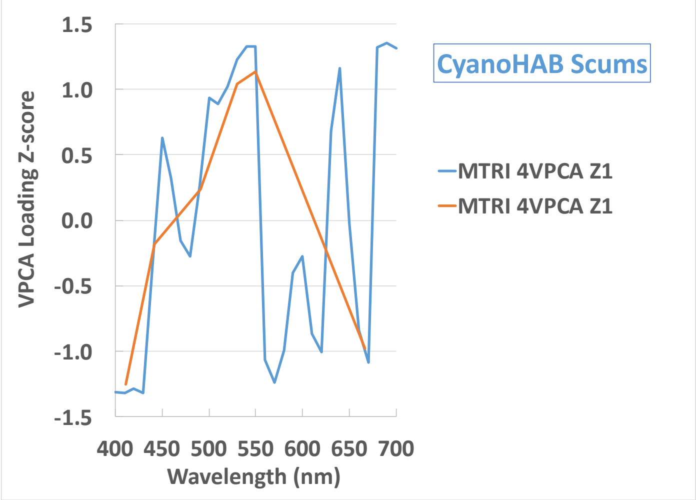

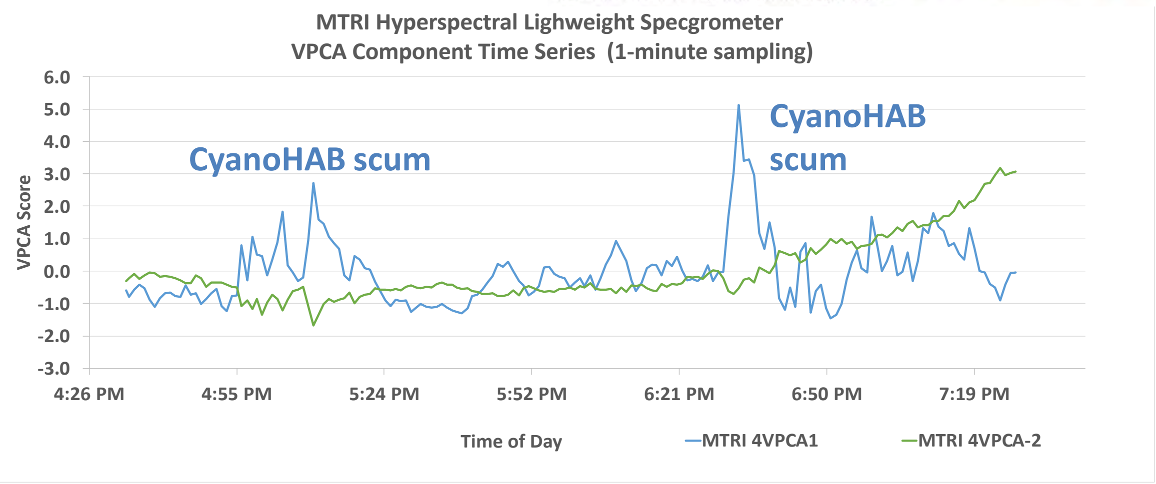

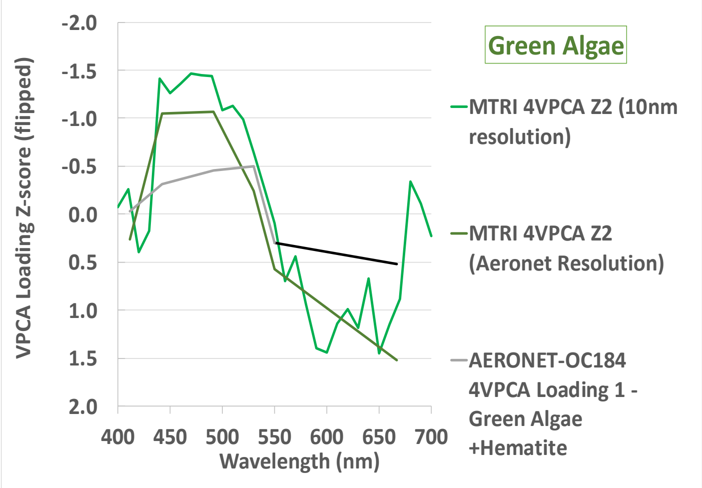

MTRI data: M. Sayer; AERONET data: Tim Moore; NOAA CI: Lake Erie HAB bulletin

Temporal changes due to phytoplankton vertical migration

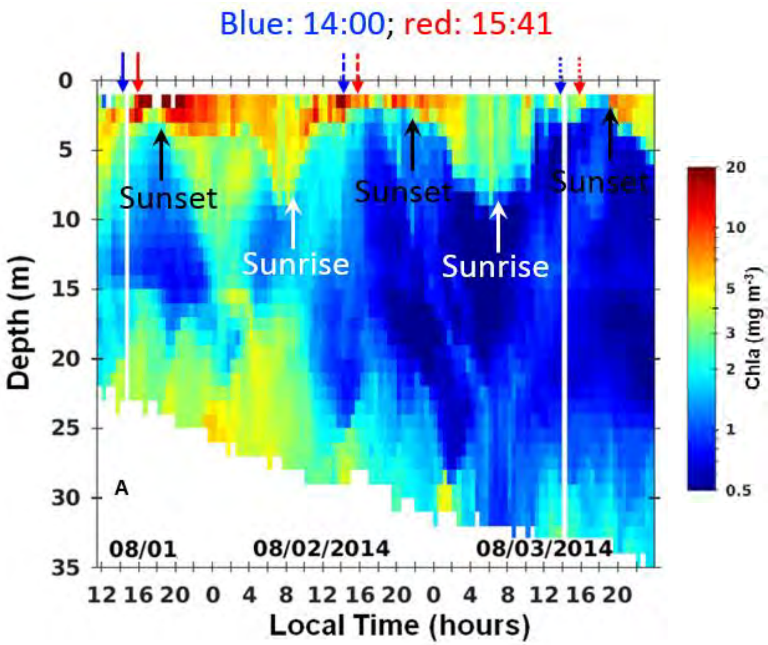

Glider measurement in red tide
(Hu et al., 2015, Harmful Algae)

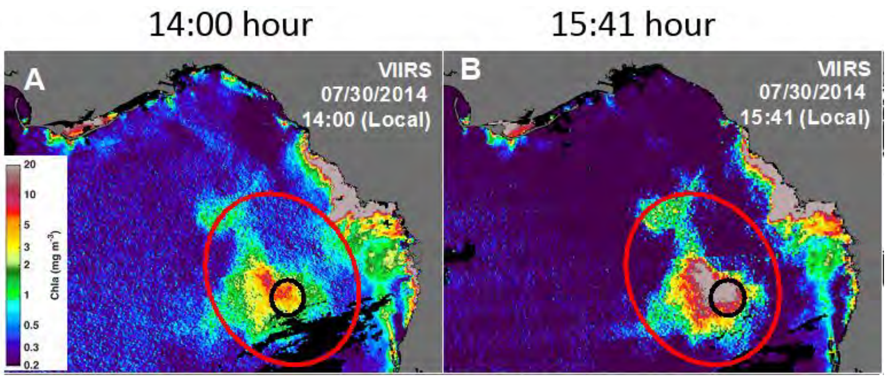

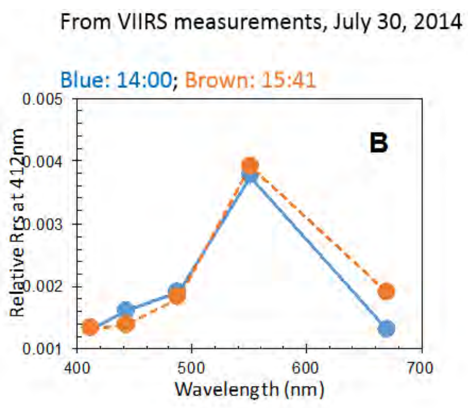

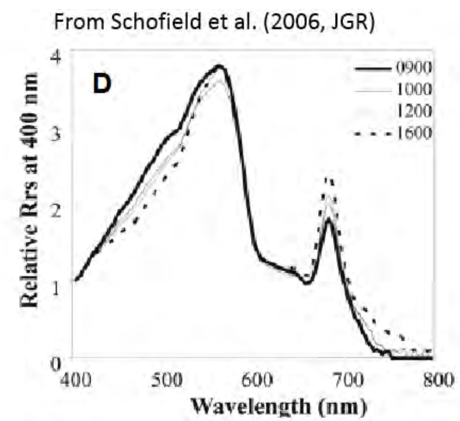

2 VIIRS measurements in the same day
(Qi et al., 2017, Harmful Algae)

More accurate analyses of primary productivity

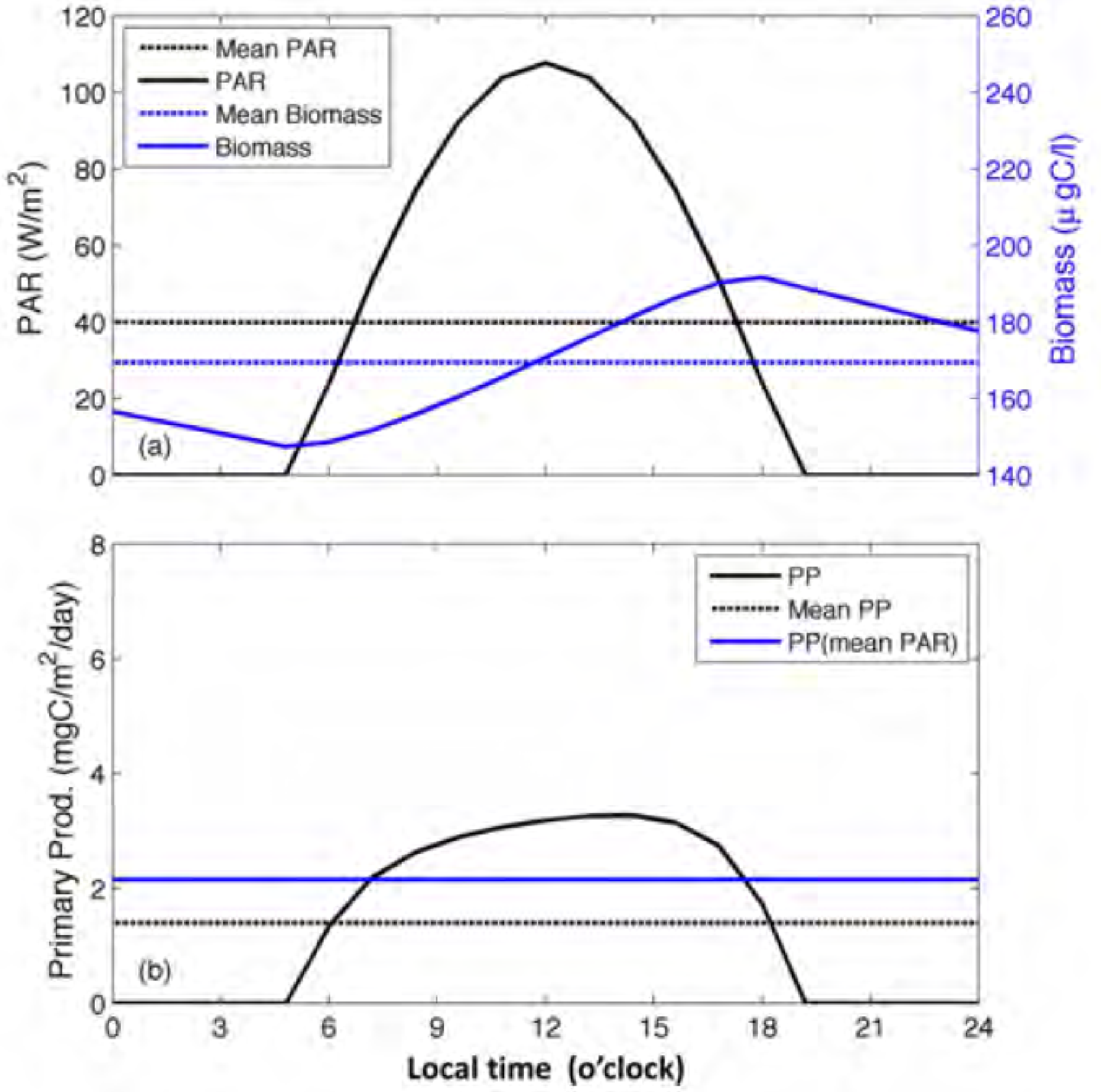

(Lee et al. 2012a)

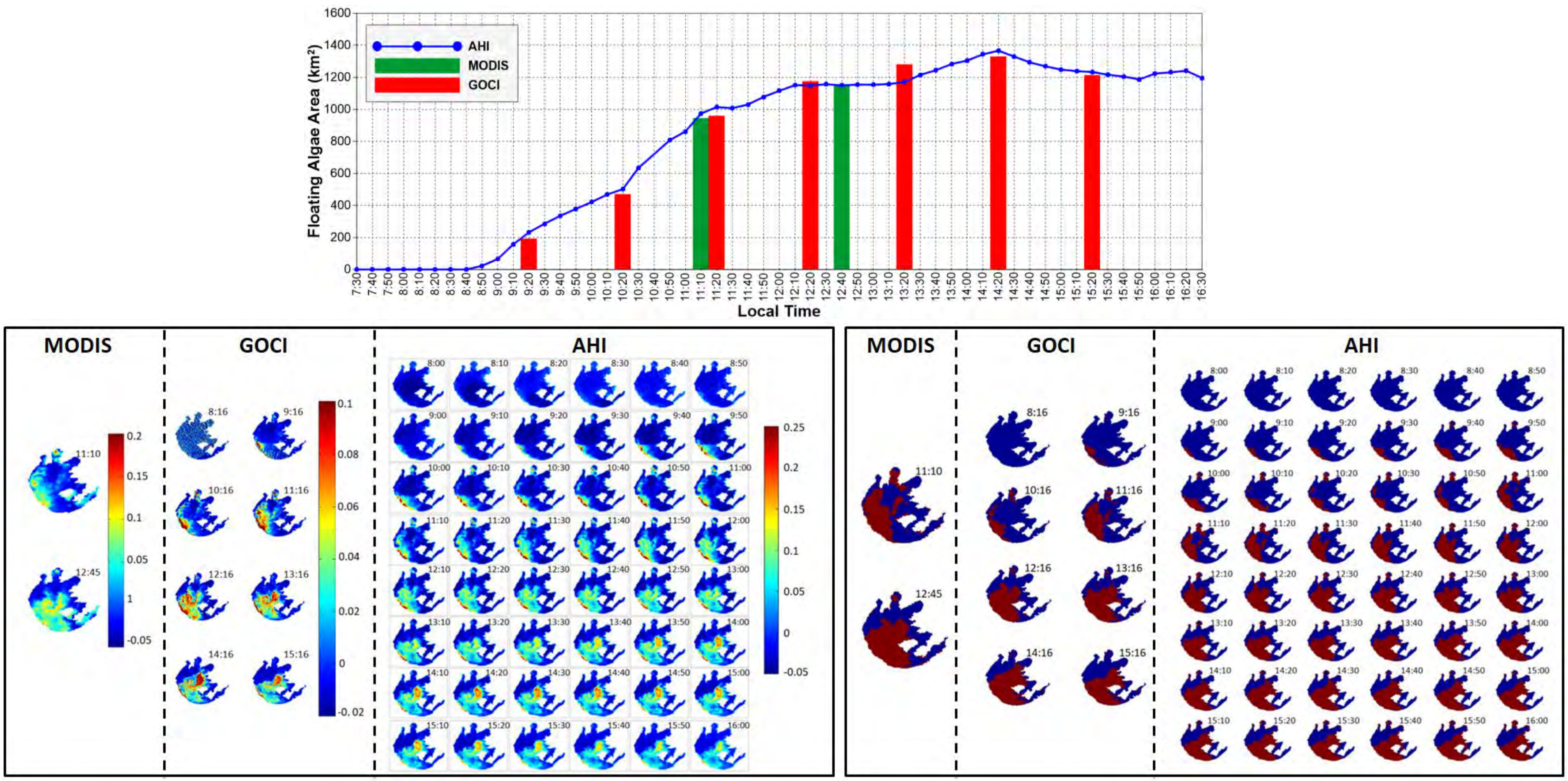

(Chen et al. 2019)

Frequency of FAI appearance

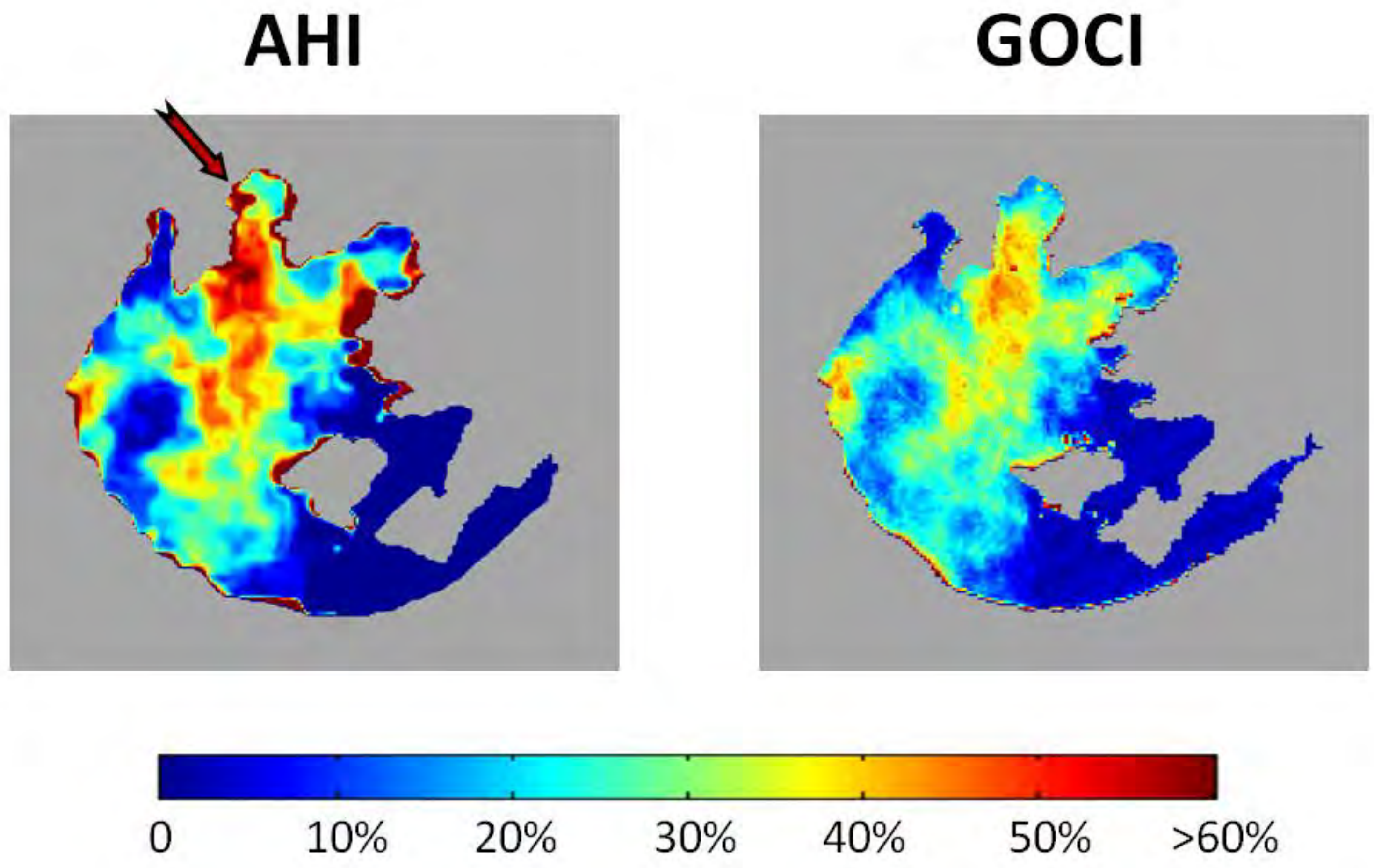

(Chen et al. 2019)

Science with high temporal resolution

"True" phytoplankton dynamics, rather advections or movements of water parcels

Impact of reduced spatial resolution

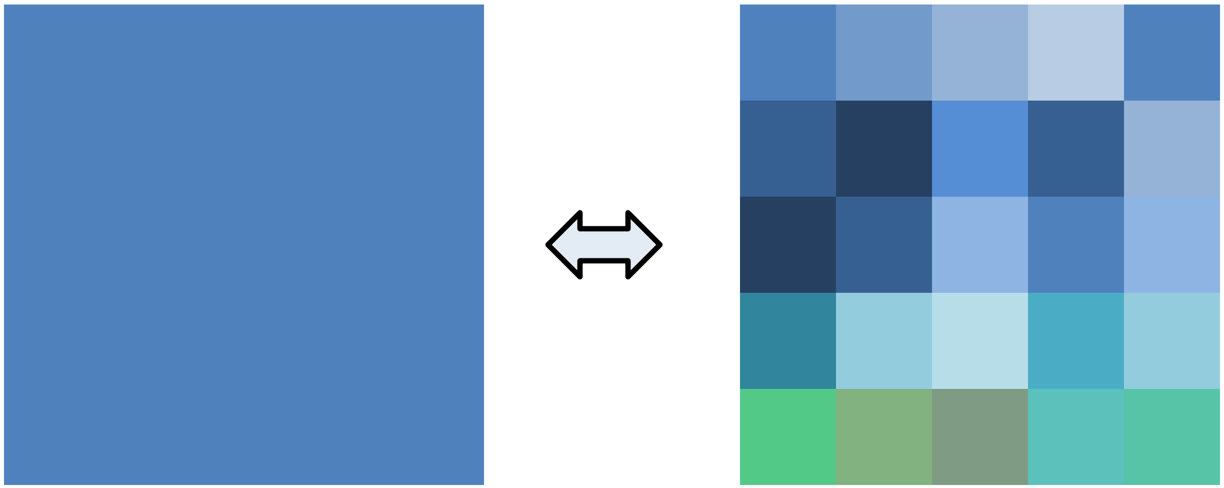

(Lee et al. 2012b)

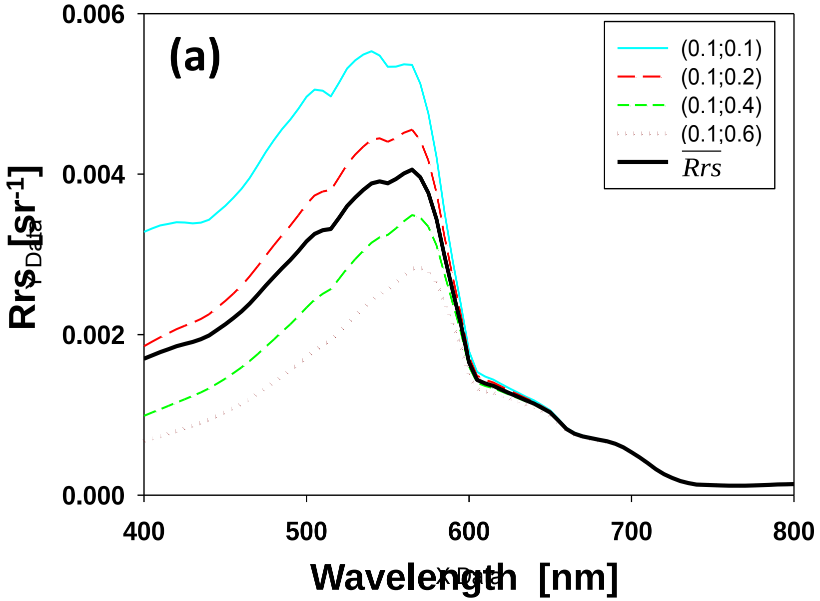

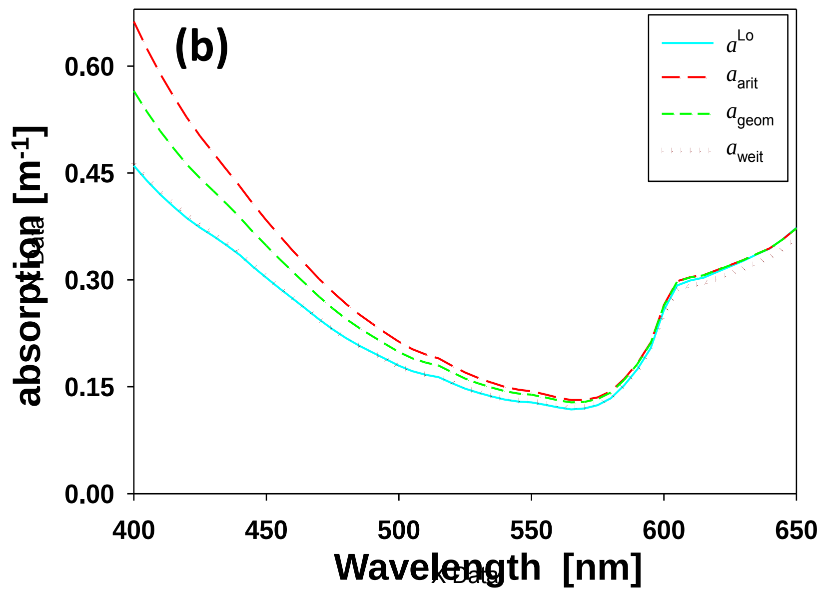

(Lee et al. 2012b)

Sea Fog (19-23 Feb. 2011)

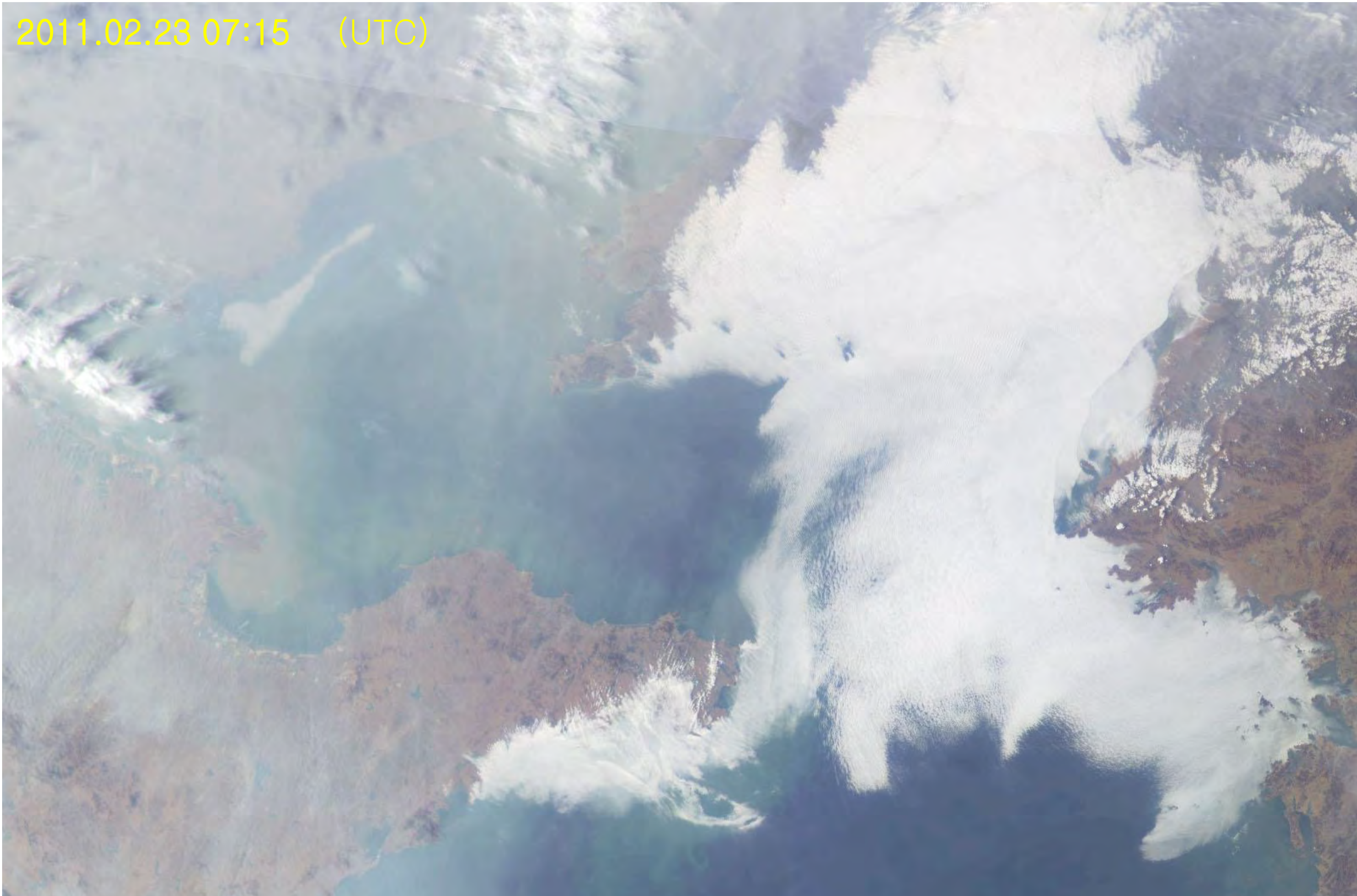

GEOSTATIONARY LITTORAL IMAGING AND MONITORING RADIOMETER

GLIMR

***Identified**: An urgent need for high frequency, hyperspectral observational capabilities for coastal ocean science, resource management, and hazard mitigation (HABs, Hypoxia, & Oil Spills)*

***Response**: **GLIMR** – a hyperspectral ocean color radiometer capable of delivery high frequency data from geostationary orbit.*

Science Goals: GLIMR develops new knowledge relevant to coastal aquatic biogeochemistry, ecosystem health, human health, and resource management advancing two major NASA Earth Science Division goals of:

- *Detecting and predicting changes in Earth's ecological and biogeochemical cycles, including biodiversity, and the global carbon cycle, and*
- *Furthering the use of Earth system science research to inform management decisions.*

GLIMR ADDRESSES KEY SCIENCE AND APPLICATIONS OBJECTIVES

Investigation Overview:

GLIMR provides...

- Science Data: 15+hours of daily observations
- Hyperspectral: UV-VIS-IR 340-1040nm
- High spatial resolution: 300m at nadir
- Fast temporal scanning: ~70 Minute GoM coverage
- Highly calibrated: Ground, On-orbit, Atmospheric Correction, & vicarious calibrations applied
- Configurable to respond to episodic events and hazards of national importance
- Societal Benefits: Economic benefits to tourism, fisheries, oil & gas, shipping, and recreational users

***1.** Short Term Coastal Processes: how high frequency fluxes of sediments, organic matter, and other materials between and within coastal ecosystems regulate the productivity and health of coastal ecosystems.*

***2.** Understanding processes contributing to rapid changes in phytoplankton growth rate and community composition.*

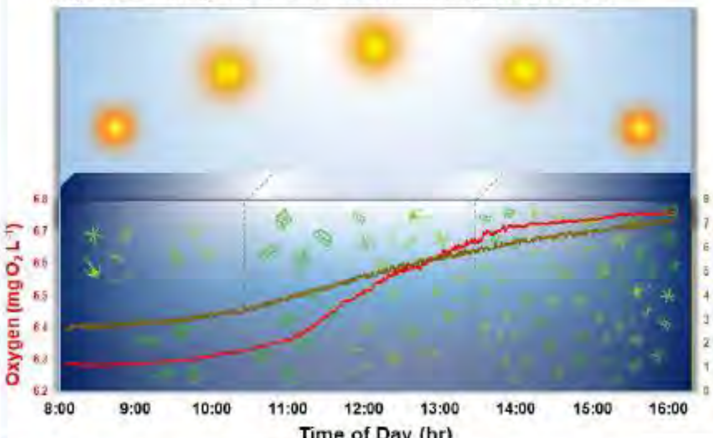

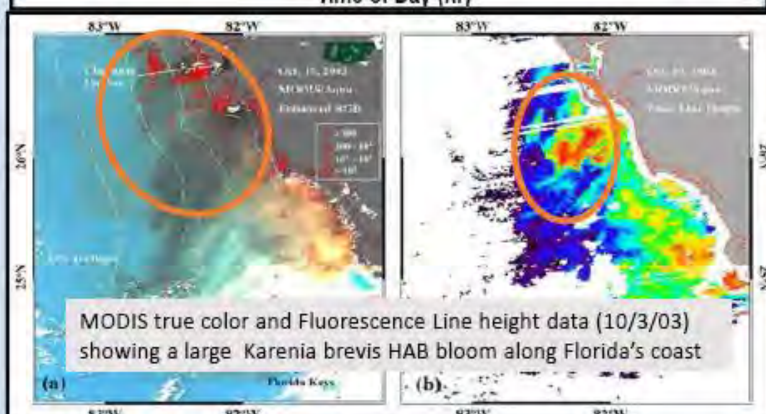

MODIS true color and Fluorescence Line height data (10/3/03) showing a large Karenia brevis HAB bloom along Florida's coast

No other sensor can achieve the degree of scientific understanding we propose with GLIMR

GLIMR provides many times more data per region per day than polar orbiting sensors!

The mean proportion of cloud-free observations during a day for polar-orbiting LEO sensors (left panel; ~0.3 to 0.6/ day in the Gulf of Mexico) based on MODIS observations between 2006 and 2011 compared to the much higher mean number of cloud-free hourly observations during a day (4 to 6/day in the Gulf of Mexico) from GOES East (right panel), based on cloud cover data between 2006 and 2011. The higher spatial and temporal resolution of GLIMR will confer a higher probability of cloud-free observations as compared to GOES and MODIS. (Red circles highlight the different scales used). Nominal location for GLIMR (98°W) is annotated in the GEO figure on right (from Feng et al. 2017).

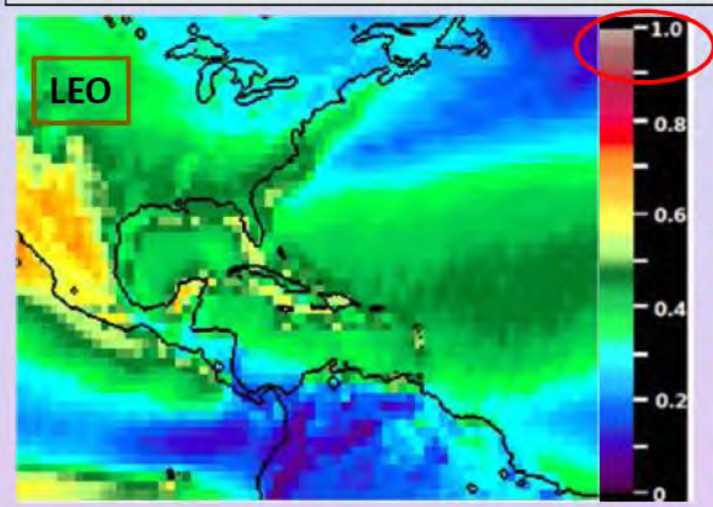

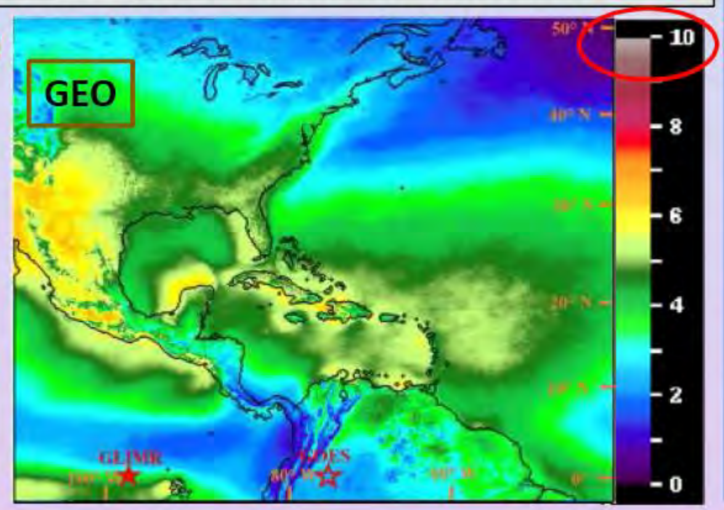

GLIMR – spatial, temporal, and spectral resolution capability uniquely suited to observing dynamic coastal ocean processes like no other current or planned mission.

Mission	Hourly Imaging	300m Spatial Resolution	Full Spectral Coverage
GLIMR	✓	✓	✓
MODIS & VIIRS			
OLCI		✓	
GOCI	✓	✓	
PACE			✓
GOES	✓		
HyspIRI (SBG ?)		✓	✓

GEOSTATIONARY LITTORAL IMAGING AND MONITORING RADIOMETER

GLIMR

Key Instrument Characteristics (CBE)

- Mass: 122 kg; Power: 156 W; Size shown at right; Data rate: 46.8 Mbps
- Spectrometer range: 340-1040 nm; 5 nm samples
- 300 m spectrometer resolution at nadir;
  330 m in Gulf of Mexico center, and
  500 m or better in all CONUS waters
- Spectrometer SNR referenced to typical spectral radiances at 42° SZA:
  - 650 for 15 nm FWHM (360-400nm)
  - 1000 for 10 nm FWHM (400-580 nm)
  - 750 for 10 nm FWHM (580-650 nm)
  - 580 for 10 nm FWHM (650-720 nm)
  - 750 for 40 nm FWHM (720-890 nm)
  - 220 for 40 nm FWHM (1020 nm)
- Landmark Imager spectral range: 555±100 nm
- 133 m Landmark Imager resolution at nadir; 146 m in Gulf
- 1.47° spectrometer cross scan FOV: 920 km swath
- 0.43° (cross scan) x 1.71° (along scan) Landmark Imager FOV
- Field of regard: 20.8° North-South and East-West in scan angle from nadir with extended field for star sensing and lunar observations
- Fully programmable scan pattern across the full field of regard that can be interrupted to cover special events
- Digital Si:PIN FPAs operating at 220 K
- Daily downlink data volume: 4 Tb
- Technology: TRL 6+ Gimbal-TRL 9
- Lifetime: 2 year mission (Class C)

High TRL of Instrument ensures Low Execution Risk

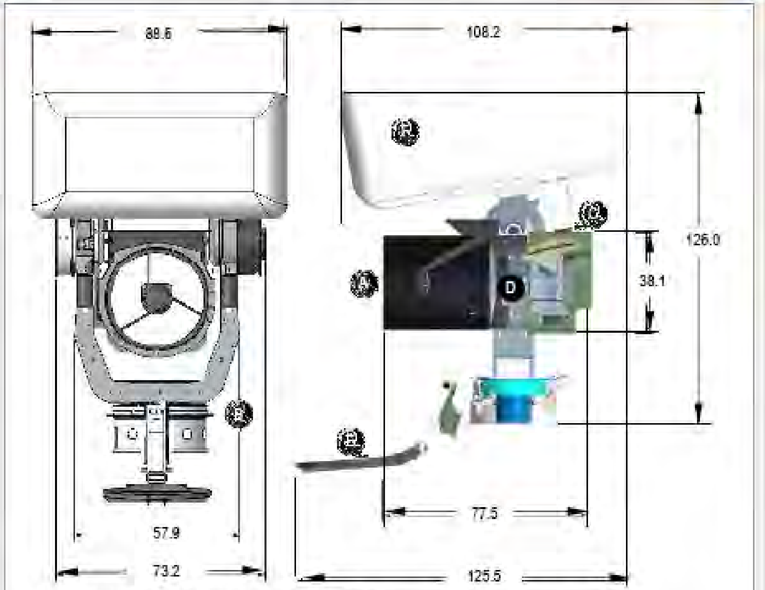

A: 28 cm, f/7.7, Cassegrain Telescope
B: Raytheon-Owned Flight Spare 2-Axis Gimbal
C: 8µm Pitch 8192×2048 SB501 FPA for Imager
D: 18µm Pitch 3072×540 SB500 FPA for Spectrometer
E: Deployable Telescope Cover
F: Thermal Radiator

All dimensions in cm

Landsat 9 OLI data processed to 145m showing the Mississippi River Delta as the GLIMR Landmark Imager will view it

Instrument
- High Resolution Hyperspectral - 141 Bands from 340 to 1040 nm
- Spectrometer and Landmark Imager in one Unit
- Fully Programmable Scan Pattern

Operation
- Geostationary Orbit on Host Satellite
- Within 88-108° W Longitude
- 3-axis Stabilized Platform
- <60Mbps Downlink
- 2 Year Lifetime
- Delivery as Early as 3/2025

Calibration
- View Vicarious Cal Sites near Hawaii, leverage proposed PACE sites if in GLIMR FOV, South Pacific clear water;
- Radiometric Cross-Calibration with VIIRS, PACE, OLCI
- Spectral Calibration using Fraunhofer Lines

Spatial-Temporal Coverage
- Full Disk Access
- Fast Revisit Time for Harmful Algal Blooms and Oil Spills
- ~70 Min Revisit for GOM

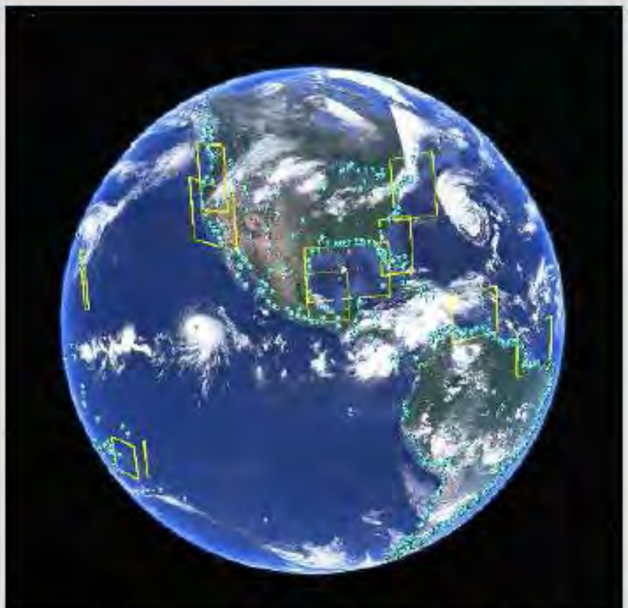

GLIMR's proposed location in GEO at 98°W offers routine access to coastal and ocean waters across a vast region stretching from the Amazon to Hawaii

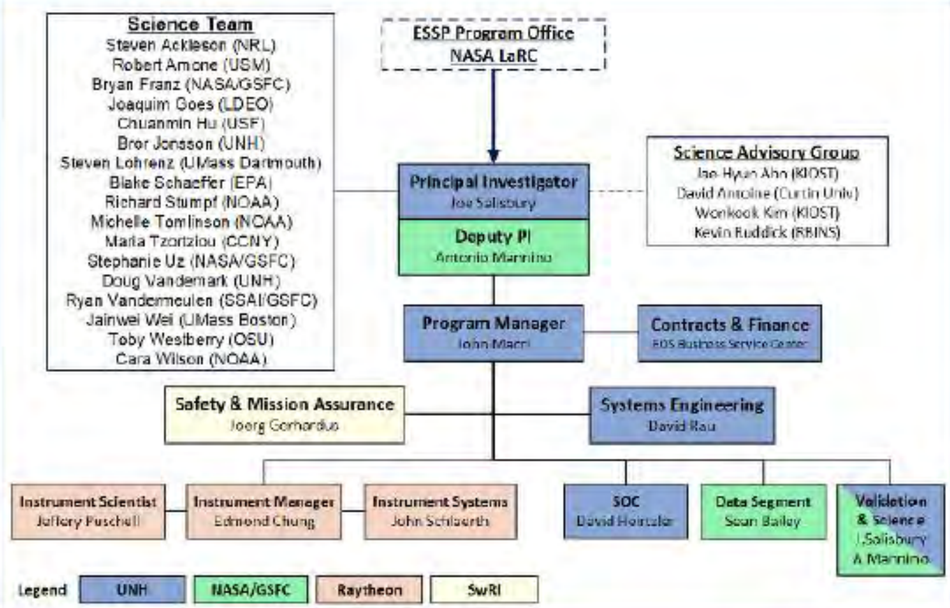

GLIMR Cost Summary	RY M$						
	Phase A	Phase B	Phase C	Phase D	Phase E	Phase F	Total
PI-Managed Mission Cost	8.74	14.52	62.12	11.40	8.66	1.78	107.22
Reserves (included in above)	1.75	2.90	12.42	2.51	1.67	0.00	21.26
Contributions	0.00	0.29	4.17	0.00	0.00	0.00	4.46
Total Mission Cost (incl. contributions)	8.74	14.82	66.29	11.40	8.66	1.78	111.67

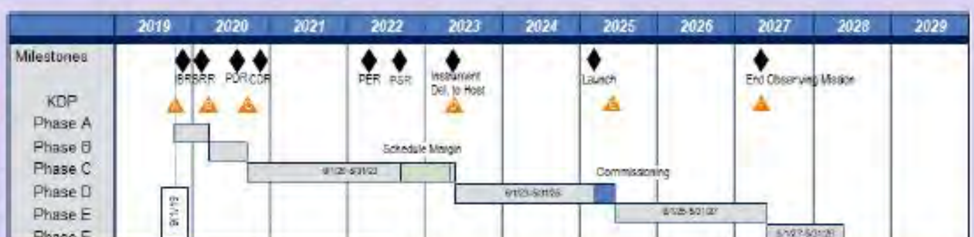

Dissolved organic matter dynamics in estuaries and their margins

Maria Tzortziou, Fang Cao, Antonio Mannino

Estuarine waters adjacent to the Blackwater National Wildlife Refuge marshes, USA

MERIS - December 2009

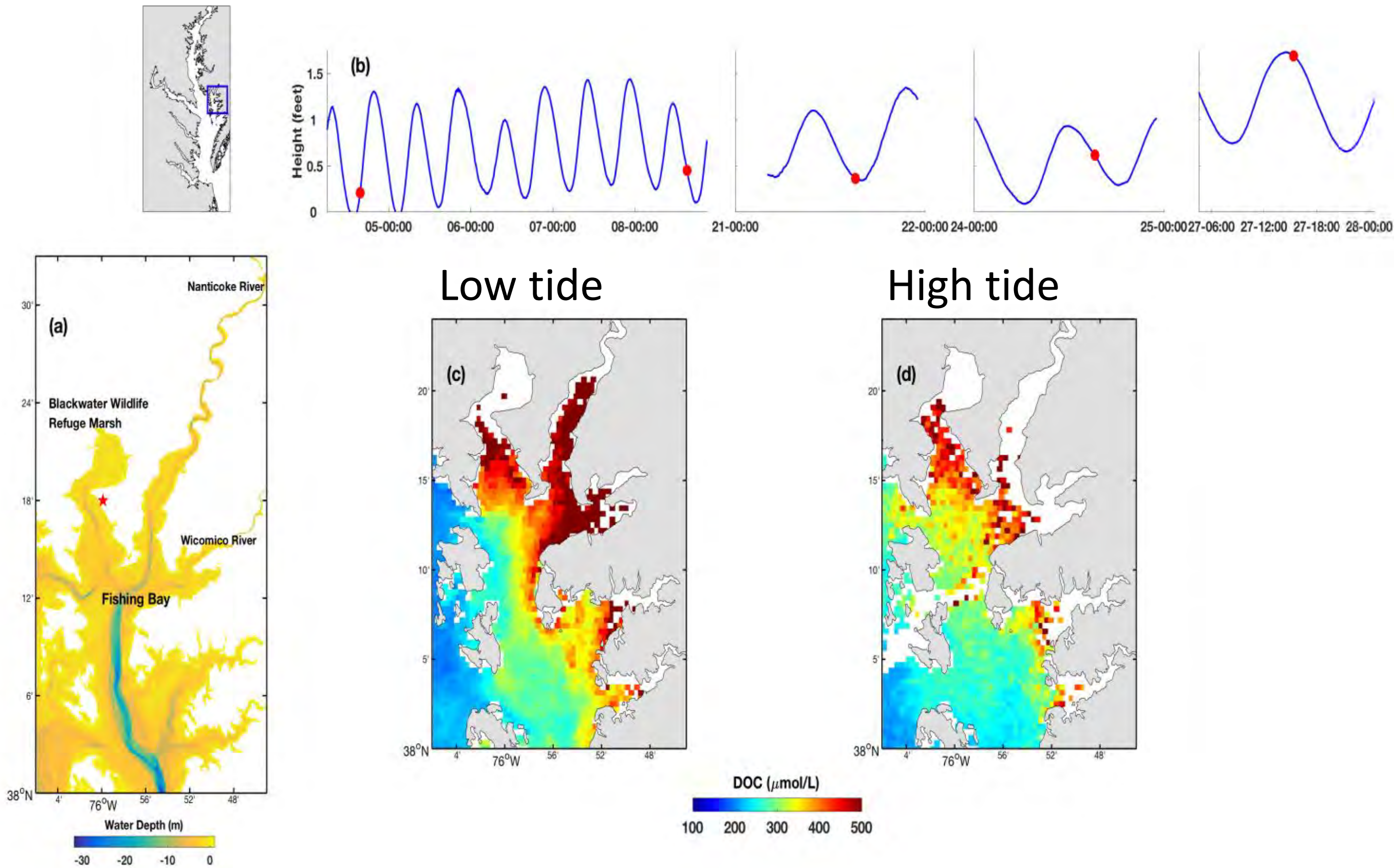

Strong impact of wetland DOC export on estuarine *Rrs*, with much higher DOC (also, higher a_{CDOM} and lower S_{CDOM}) retrieved using satellite imagery collected at Low Tide (left panel) compared to High Tide (right panel)

Dynamics of atmospheric trace gases and aerosols in Korean coastal waters and impacts on Ocean Color retrievals

Maria Tzortziou, Owen Parker, Brian Lamb, Nader Abuhassan, Jay Herman, Bob Swap

Measurements over land and ocean

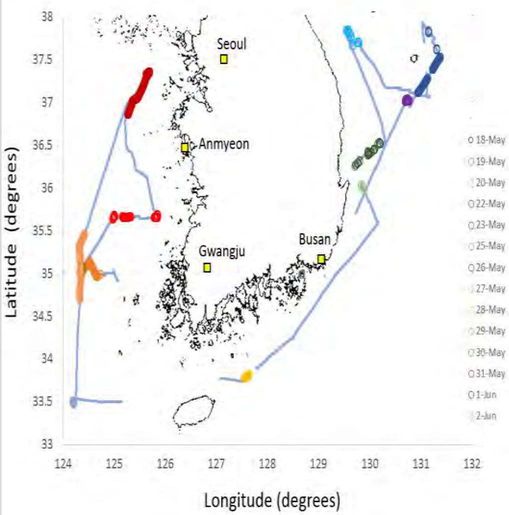

Total Column (TC) O_3 and NO_2 variability

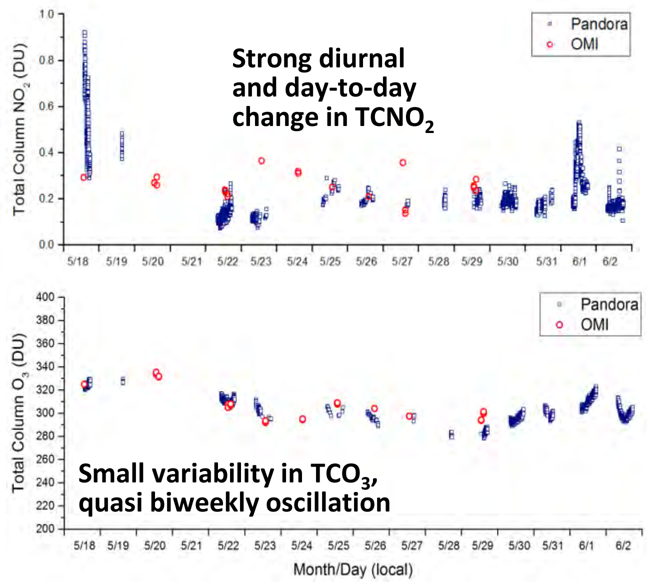

Impact on ocean color retrievals

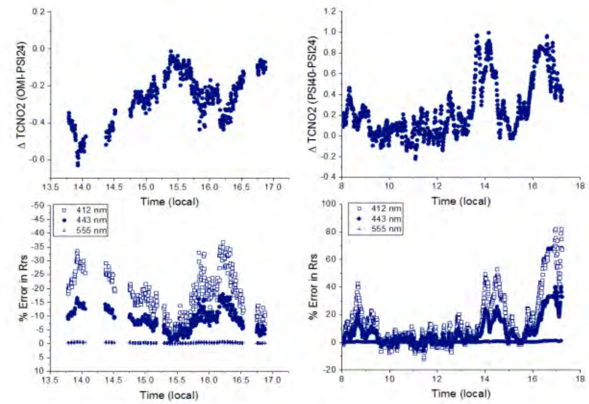

Difference in $TCNO_2$ between shipboard Pandora and OMI on May 18 2016 and resulting false diurnal variability (%) in ocean R_{rs}

Difference in $TCNO_2$ over coastal land and coastal ocean offshore Seoul and resulting false diurnal variability (%) in ocean R_{rs}

Results:

• **$TCNO_2$ highly variable over the ocean**: reached 0.9 DU near Busan, and >0.5 DU offshore Seoul (>50 km)

• Emissions over the land considerably affected $TCNO_2$ dynamics over the ocean, but in complex ways and often resulting in very different temporal patterns between coastal land sites and offshore coastal waters.

• **Satellite OMI NO_2 retrievals:** underestimate NO_2 near hotspots, overestimate NO_2 in 'rural'/clean areas, and do not capture the strong spatial/temporal variability relevant to high-spatial and high-temporal resolution ocean color sensors.

• **Satellite OMI O_3 retrievals:** very consistent with shipboard measurements over coastal ocean, because total column ozone variability is mostly driven by larger scale meteorological processes and synoptic weather fronts that were captured successfully in the relatively coarse satellite imagery from Aura OMI.

• **Large impacts of $TCNO_2$ variability on ocean color retrievals:** 40-80% error in Rrs

Can GOCI data be used to retrieve photosynthetic parameters?

ipar versus hourly change in chlorophyll

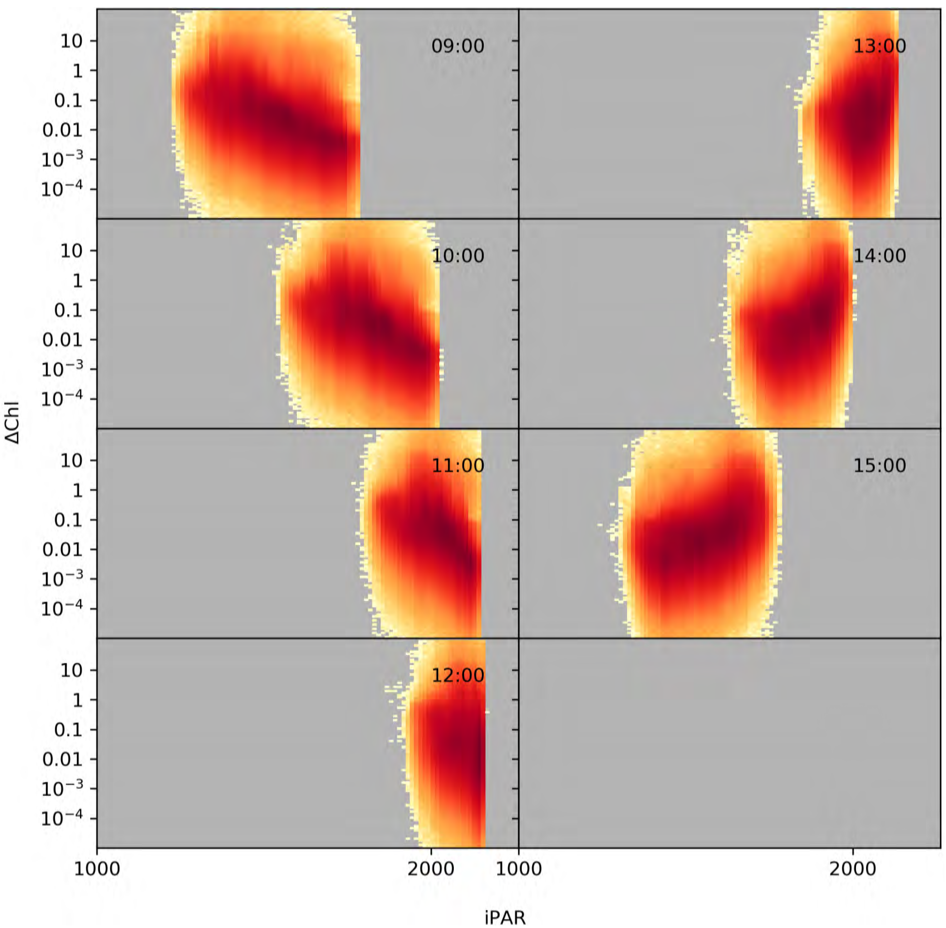

ipar versus ϕ_{sat}

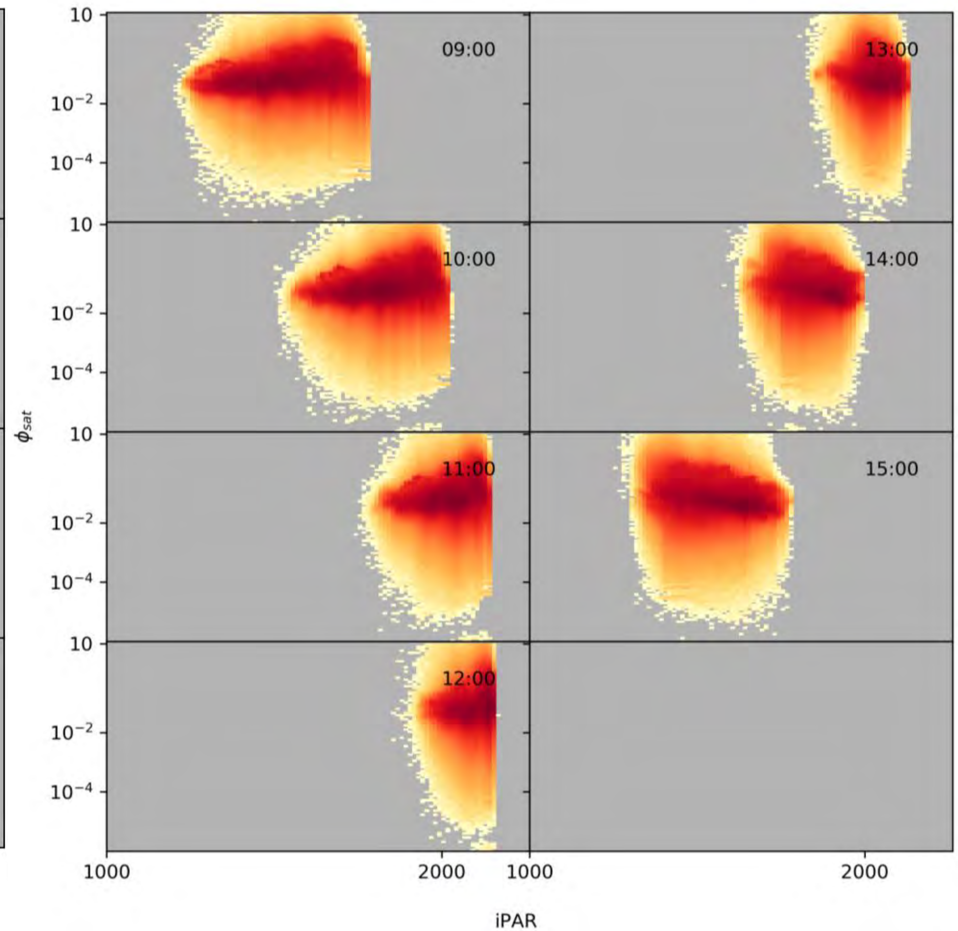

Salisbury, Jonsson, Mannino, Kim et al.

$$b_b^{\ Lo} \approx \overline{b_b^{\ Hi}(i)}$$

$$a^{Lo} \approx \frac{n\, b_b^{\ Lo} \prod_{i=1}^{n} a^{Hi}(i)}{\sum_{i=1}^{n} \left(b_b^{\ Hi}(i) \prod_{j=1,\, j \not\subset i}^{n-1} a^{Hi}(j) \right)}$$

(Lee et al. 2012b)

A fundamentally different approach may be enabled using high frequency (geostationary) data

Constraining the biological perturbation of CO_2 via tracking particle inventories in a Lagrangian context.

Jonsson, Salisbury, Mahadevan, Campbell (2009)
Jonsson, Salisbury, Mahadevan (2011)
Jonsson, Salisbury (2016)

Premise:

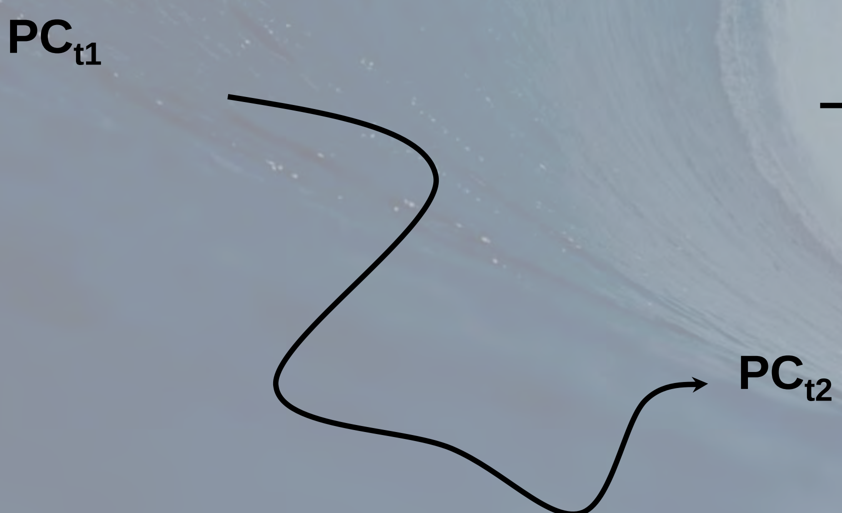

$$\frac{(PC_{t2} - PC_{t1})}{(t2 - t1)} \approx \text{bio perturbation of } CO_2$$